CHALMERS
UNIVERSITY OF TECHNOLOGY

A conceptual model for how to design for building envelope characteristics. Impact of thermal comfort intervals and thermal mass on commercial

Journal of Building Engineering xxx (xxxx) xxx

Contents lists available at ScienceDirect

Journal of Building Engineering

journal homepage: http://www.elsevier.com/locate/jobe

A conceptual model for how to design for building envelope characteristics. Impact of thermal comfort intervals and thermal mass on commercial buildings in U.S. climates

Carl-Eric Hagentoft [a,*], Simon Pallin [b]

[a] Chalmers University of Technology, Division of Building Technology, Department of Architecture and Civil Engineering, Chalmersplatsen 4, Gothenburg, 41296, Sweden
[b] Oak Ridge National Laboratory, Building Envelope & Urban Systems Research Group, Energy and Transportation Division, 1 Bethel Valley Rd, Oak Ridge, TN 37830, USA

ARTICLE INFO

Keywords:
Energy demand
Conceptual model
Lumped model
Network
Thermal mass
Building envelope performance

ABSTRACT

The paper presents a simplified conceptual model for energy demand calculations based on building envelope characteristics, thermal mass and local climate. It is based on a network model and lumped analysis of the dynamic process. Characteristic parameters for the buildings are suggested; Driving temperature (DT), Driving temperature difference, (DTD), External Load Temperature (ELT), and Thermal Load Resistance (TLR). The Building Envelope Performance (BEP^0), based on a controlled constant indoor temperature is introduced. Solution techniques using stable explicit forward differences based on analytical solutions are derived. The conceptual model has been used for mapping the Driving temperature difference and introduced two performance factors α and β. The first factor represents the effect of thermal comfort interval and thermal mass on the energy demand. The latter represents the ratio between cooling and heating energy demand. These three parameters and factors have been visualized on U.S. maps and enable a possibility to communicate the demand of energy, and cooling and the coupling to building characteristics, in a concise way.

1. Introduction and background

The energy balance of buildings has been studied intensely for many decades using both analytical and numerical tools. There are several standards [1,3]; [4,34], and computational tools [5,8,9] to assess the overall energy performance of buildings. Due to a complex interaction between building characteristics, outdoor climate, building usage, HVAC equipment, occupants' indoor climate preferences, etc., describing the thermal performance of a building using performance indicators, metrics, and ratings is difficult. Still, metrics exist to describe single building characteristics variables, such as *R*-value, U-factor, airtightness (ACH50/75), and Solar Heat Gain Coefficient (SHGC). However, it is well known that neither the *R*-value [10], nor any of the other indicators can fully, or even realistically, solely describe the overall building thermal performance and response.

Various attempts and research have been conducted to define metrics and performance indicators which account for most variables that possess a significant impact on the overall building energy performance [11]. Reilly and Kinnane tried to separate out the effect of thermal mass in energy simulations by taking the ratio of the energy demand in a dynamic model to that calculated using a quasi-static model [12]. They defined that measure as the transient energy ratio, TER. Alterman et al. took a different approach to try and develop a holistic measure of the building envelopes performance [13]. In studying the effect of thermal mass on the performance of the building's energy demands, field measurements showed that similar internal conditions could be obtained for walls with significantly different steady state *R*-values. This led to the development of an approach to quantify or capture all the effects or properties of the wall including the effect of climate in one value defined as the dynamic temperature response or T value. The T value is a function of the dynamic profiles of the exterior climate and the response of the building's internal temperature. Building on the work of Alterman et al., Arkar and Perino developed a metric based on the T value to account for the dynamic response of what they refer to as adaptive materials in the building envelope, such as phase change materials [2]. Instead of measuring the dynamic temperature profiles, they used the envelopes inner surface heat flux, and the sol-air temperature [14] for exterior boundary condition. Arkar and Perino presented a U dynamic

* Corresponding author.
E-mail addresses: carl-eric.hagentoft@chalmers.se (C.-E. Hagentoft), pallinsb@ornl.gov (S. Pallin).

https://doi.org/10.1016/j.jobe.2020.101994
Received 26 June 2020; Received in revised form 3 November 2020; Accepted 5 November 2020
Available online 11 November 2020

thermal performance metric which was calculated using a linear fit to the daily thermal response through the origin and effectively captured the effect of thermal inertia. Their work claims that U dynamic thermal performance metric could be used to replace the U-factor in the calculation of envelope transmittance.

In the 1970s, the M-factor was presented with the intent to represent the effect of thermal mass on the performance of the building envelope that was not reflected in or accounted for by the steady state *R*-value [15,16]. The M-factor was defined as the ratio of the dynamic heat flux of the masonry wall to theoretical steady state values and was used as a correction factor to the steady state conduction equation to account for thermal mass.

Christian and Kosny introduced the dynamic benefit for massive systems [10], referred to as DBMS. This approach took into consideration the materials that comprised the building envelope and its configuration. In their study, climate conditions were accounted for and an equivalent *R*-value was determined by comparing the thermal dynamic behavior of massive walls and light wood-framed walls exposed to the same climate. Kosny et al. showed that thermal mass does play a role and depends on both the configuration of the wall and exterior climate. According to their work, the impact of mass is greater in hot climates than for cold climates. The same approach would later be used to quantify the benefits of green roof systems [17]. Using a similar approach, Moody and Sailor showed the dynamic benefits of green roofs using the DBGR. Their work showed the dependence of climate zone on the utility of green roofs relative to conventional roofs with equivalent steady state *R*-values.

Despite thermal mass having been repeatedly proven relevant for the overall building energy demand, some studies claim otherwise. As a response to the introduction of the M-factor, Childs and Godfrey et al. [18] presented studies which claimed that thermal mass in buildings was insignificant [7,19]. The reason these studies did not see any benefits of internal mass was because the indoor temperature conditions were fixed at 20 °C [68 °F]. More recent studies show that even though the mass of the building envelope is relevant for fluctuations in exterior temperatures for relatively short time periods [20], measurements made over longer periods, a day or more, proved building envelope mass insignificant. Godfrey et al. did not study the impact of the building interior mass and concluded that to attribute the effect of thermal mass to walls, solely, was incorrect and that other factors needed to be considered such as solar loads, internal loads, and the transient response to meet the energy demands required to maintain thermal comfort.

There are also various simplified methods to calculate heating and cooling loads in buildings from estimating the overall thermal performance of buildings, such as CLTD/CLF [4] and the RTS method [21]. These methods include all variables relevant to the energy demand in buildings, including interior loads from solar radiation through windows. However, these methodologies do not present single indicators or metrics that represent the whole building energy performance. Previous ASHRAE work from 1975 presents an approach to quantify the thermal performance of the building envelope in air-conditioned buildings by introducing the concept of overall thermal transfer value, OTTV [22]. OTTV is defined as the maximum thermal transfer permissible in the building through its walls or roof due to solar heat gain and outdoor – indoor temperature differences. OTTV has been adopted in the building codes in several ASEAN countries with modifications throughout the years [23]. Later, ASHRAE abandoned the approach because of its limitation as a measure to account for internal loads and decided to treat the impact of each of the properties separately through the implementation of whole building energy calculations with additional properties such as thermal inertia and air infiltration in the revision ASHRAE 90.1–1989 [24].

This study focuses on the energy use for commercial buildings in U.S. climates. The aim is to develop a conceptual model, a simplified tool, based on network and lumped analysis that is graspable, visual, and simple to use “as-is” or in new tools to be developed. This is achieved by simplifying the otherwise complex energy balance of a building and studying the thermal response of buildings. While keeping a building unconditioned, the outdoor climate induced fluctuation in interior temperature is evaluated to find the overall energy demand. Such an approach allows the study of the thermal performance of temperature-controlled buildings independently of the exact use of the building. Using methods presented in previous work ([25,26], this paper presents conceptual models and energy performance indicators that enable an overall and holistic understanding of the main processes and parameters that govern the thermal performance of buildings. These models and performance indicators can be used for the development of hour to hour calculations of the effect and energy needed during the year. Additionally, these models can be used for heating and cooling demand calculations, and in evaluating the thermal performance of the building envelope. The work of this paper also supports the development of the Oak Ridge National Laboratory initiated DOE Building Envelope Campaign [6], to support commercial building owners in making building envelope energy efficient design decisions for both new constructions and retrofits. Using an embedded energy assessment tool that is based on some of the models presented in this paper, participants of the campaign are able to evaluate the overall building envelope thermal performance using the BEP metric [27].

The result of this paper is presented using DOE prototype buildings [28] and generated maps representing U.S. climates in order to visualize the importance of the building envelope design, thermal comfort interval, and thermal mass of commercial buildings.

2. Energy balance

The energy balance of a building is governed by various heat flows and heat capacities in a building and its components. The driving force for these energy transfer mechanisms are temperature changes between the outdoor and indoor air, surface temperatures, air pressure gradients, sky temperatures, and solar radiation.

For the sake of simplicity and to avoid unnecessary computational efforts from too many details of geometric origins, the complex and rather complicated interaction between a building and its surroundings needs to be simplified. For instance, the exact wind pressure and velocity at surfaces can be simplified in order to be able to grasp the problem in its entirety. Here, equivalent temperatures are used that make it possible to get a reasonably good approximation of what happens at the building exterior surfaces and its impact on the heat transfer. We also assume that the solar gains can be calculated based on available solar models [29] and the geometric issues due to the orbit of the earth around the sun around are dealt with in a reasonably accurate fashion. An hourly weather data year with radiation data, together with window areas and orientation, are assumed to be sufficient for these calculations. For air leakage, wind and buoyancy driven building air infiltration is estimated using Effective Air Leakage area and simplified method presented in ASHREA Fundamentals Chapter 16.10 [30]. Though, other methods to predict air leakage could have been applicable for this study, the actual air leakage rate and the impact of the same are of most relevance for this work. The overall conceptual model of this paper is further elaborated in Fig. 22.

For this study, we assume the indoor temperature to be uniform throughout the interior space. In reality, there might be some differences due to window emitted solar radiation and the placement of air distributors. However, such an assumption is justified for the sake of simplicity and the goal of getting reasonably good estimates for the overall energy demand. In addition, no distinction is made between convective heat transfer and long wave radiation exchange between interior surfaces and the indoor air. Moisture transfer and effects of latent heat are also neglected.

The heat transfer through the building envelope is described by U-values, air infiltration rate, and solar transmittance (SHGC) through windows. In the latter heat transfer process, the results of this study rely

on a simple and constant SHGC factor independent on solar incident angles. The effect of more complicated shading devices and self-shading of the building are not accounted for.

The conceptual heat transfer model developed relies on one thermal mass lump or node as will be discussed in detail throughout this paper. The presented model has been successfully validated against EnergyPlus and WUFIPlus [26].

2.1. Heat flows

Fig. 1 depicts the overall building thermal processes to be studied. The interior temperature, $T_i(t)$ (°C [°F]) is governed by the various heat transfers to the interior through the opaque building envelope Q_t(W [Btu/hr]), window transmission,Q_W (W[Btu/hr]), air infiltration Q_v(W [Btu/hr]), solar Q_{sol}(W[Btu/hr]) and internal gains Q_{gain}(W[Btu/hr]), as well as the resulting heat and cooling load Q_{HC} (W[Btu/hr]) to maintain the indoor temperature. Since the indoor temperature is varying according to applied temperature control system setpoints, the interior thermal mass cM_0(J/K[Btu/°F]) is of interest for this process.

The exterior ambient air temperature is denoted by $T_e(t)$ (°C [°F]). The exterior equivalent temperature, accounting for convection and radiation exchange with the exterior building envelope surface is denoted by $T_{eq}(t)$ (°C [°F]). The air infiltration rate,R_a (m^3/s[cfm]), does normally vary over time but can, for the purpose of simplification, be considered constant.

The air infiltration heat transfer is:

$$Q_v(t) = R_a(t)\cdot\rho_a c_{pa}\cdot(T_e(t) - T_i(t)) = K_v(t)\cdot(T_e(t) - T_i(t)) \quad (1)$$

Here, $\rho_a c_{pa}$(J/m^3,K [Btu/ft^3,°F]) is the volumetric heat capacity of air at constant atmospheric pressure. The heat transfer through windows is:

$$Q_W(t) = \sum_{m=1}^{M_W} A_{W,m}U_{W,m}(T_e(t) - T_i(t)) = K_W\cdot(T_e(t) - T_i(t)) \quad (2)$$

Here, M_W is the total number of windows. The U-value of the window number m is $U_{W,m}$ (W/m^2,K[Btu/ft^2,hr,°F])) and the corresponding area is $A_{W,m}$ (m^2[ft^2]). Equations (1) and (2) also define the thermal conductance K_v (W/K[Btu/hr,°F]) for the air infiltration and K_W (W/K [Btu/hr,°F]) for the transmission through all of the windows.

The temperature dependent transmission gain Q_t, through the remaining opaque building envelope can be found with high accuracy through response analysis [25] or through numerical methods using discretization and time stepping methods.

By introducing a corresponding heating and cooling sink to the interior, Q_{HC}, the indoor temperature can be maintained within the acceptable thermal comfort interval.

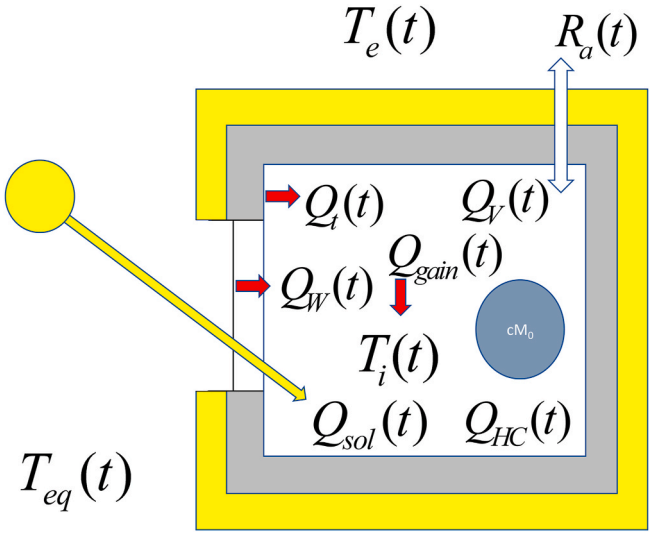

Fig. 1. Temperature process of a building including heat sources and surrounding external air and equivalent temperatures.

2.2. Network model and superposition

Superposition is used in the following analyses in order to divide the thermal process into two parts. The solution is exact if linear processes are followed. This requires that air infiltration rate is constant or a function of time. Fig. 2 illustrates a finite difference method, FDM. The wall structure is modelled as a series of lumped masses, representing the heat capacity of each numerical cell, and conductances in between these masses representing the thermal coupling between each cell. The building envelope components are indexed $1 \le j \le J$ and the number of numerical cells for building envelope component j is N_j. The mass of the numerical cell i in building envelope part indexed j is denoted m_{ji}(kg [lb]) and its heat capacity is c_{ji}(J/K,kg [Btu/°F,lb]).The building envelope surface area is denoted by A_j(m^2[ft^2]). The thermal conductance between the interior and the first numerical cell in building envelope part j is denoted $K_{j,1}$(W/K[Btu/hr,°F]). It accounts for both half the thermal resistance of the first numerical cell as well as the interior surface resistance. The corresponding thermal conductance between the exterior and the last numerical cell is denoted K_{j,N_j+1} (W/K[Btu/hr,°F]).

First, we define a base case (denoted "0") with an applied heating and cooling demand, $Q^0_{HC}(t)$, that equals the net flow to the interior, while the interior temperature is kept constant $\overline{T}_i$ (see Fig. 3). This is the temperature which represents the mid setpoint temperature below. For this case, the thermal mass of the interior does not play any role in this process since the interior temperature is fixed.

The base heating and cooling effect,$Q^0_{HC}(t)$ resulting in a constant interior temperature, is used as a first estimate of the heating and cooling demand.

The remaining thermal process is shown in Fig. 4.

By choosing an appropriate $\Delta Q_{HC}(t)$, the peak and overall energy demands can be minimized. However, within a limited degree of freedom stated by the setpoint temperature constrain in Eq. (3).

$$-\Delta T/2 \le T_i'(t) \le \Delta T/2 \quad (3)$$

Here, ΔT, represents the temperature deadband width.

3. Conceptual network model

In order to simplify the networks introduced in Section 2, two important simplifications are introduced in this section. A Conceptual network model is introduced, and important Characteristic parameters are defined.

3.1. Defining the networks used

In this subsection a simplified conceptual network is suggested, compared to the comprehensive network in Fig. 2. In the original network the calculation of the heat transfer through the layered envelope parts can be arbitrarily accurate, relying on finer discretization. Here, we instead make it simpler using quasi-steady state calculations. Furthermore, the thermal mass of the building envelope on the interior side of the insulation is accounted for by being added to the interior mass. Fig. 5 shows the suggested conceptual simplified network in two alternative ways.

The U-value of building envelope component j is denoted U_j(W/m^2,K [Btu/ft^2,hr,°F]), it includes all thermal resistance inside the envelope part as well as the surface resistances at the exterior and interior surface. cM (J/K[Btu/°F])) represents the heat capacity of the interior including the inner wall layer of the building envelope. The total mass of this inner

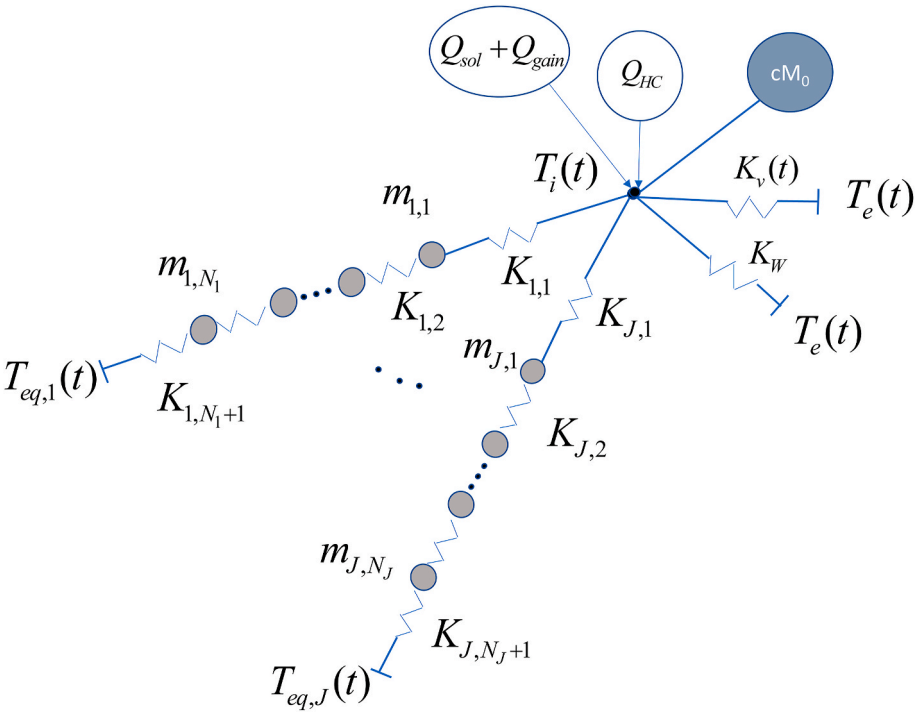

Fig. 2. Thermal network model of a building. The small black dot represents the interior temperature. The gray filled circles represent the thermal mass of the numerical computational cells. The blue filled circle represents the interior thermal mass of the building. (For interpretation of the references to colour in this figure legend, the reader is referred to the Web version of this article.)

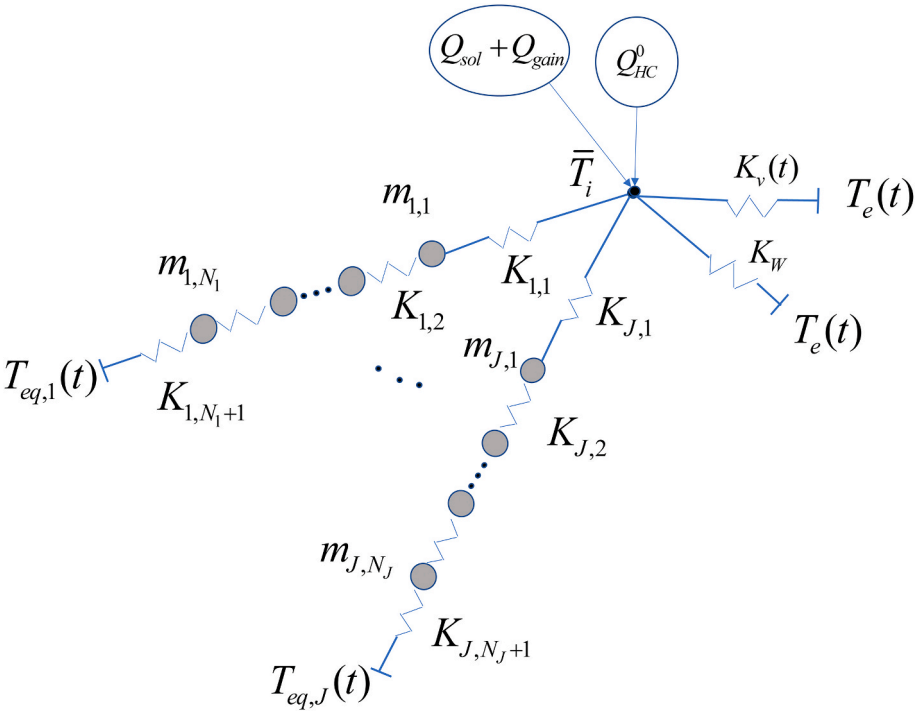

Fig. 3. The base effect,$Q^0_{HC}(t)$(W[Btu/hr]), is the net energy to the interior node required to keep the indoor temperature constant and equal to, $\overline{T}_i$, i.e. the mid setpoint temperature.

layer of envelope part j is denoted $M_{j,1}$.

$$cM = cM_0 + \sum_{j=1}^{J} c_{j,1} M_{j,1} \tag{4}$$

Thermal mass on the exterior side of the building envelope are neglected. Justification of this is made in the appendix.

Opposite to FDM calculations, the network depicted in Fig. 5 instead approximates the flow through the walls using a quasi-steady-state approach. Thus, the heat flow will be different than the previously heat flow, $Q_{HC}(t)$, presented in Fig. 2. The new heat flow is denoted using

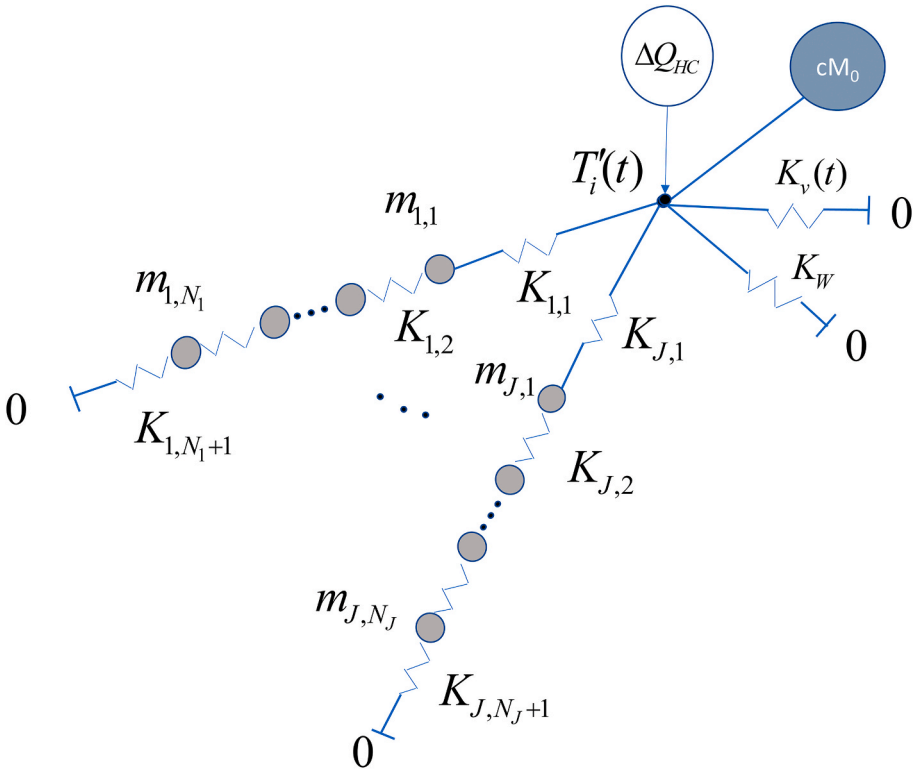

Fig. 4. Added effect, $\Delta Q_{HC}(t)$ (W[Btu/hr]), to the interior node in order to keep the interior temperature within the thermal comfort interval $-\Delta T/2 \leq T_i'(t) \leq \Delta T/2$.

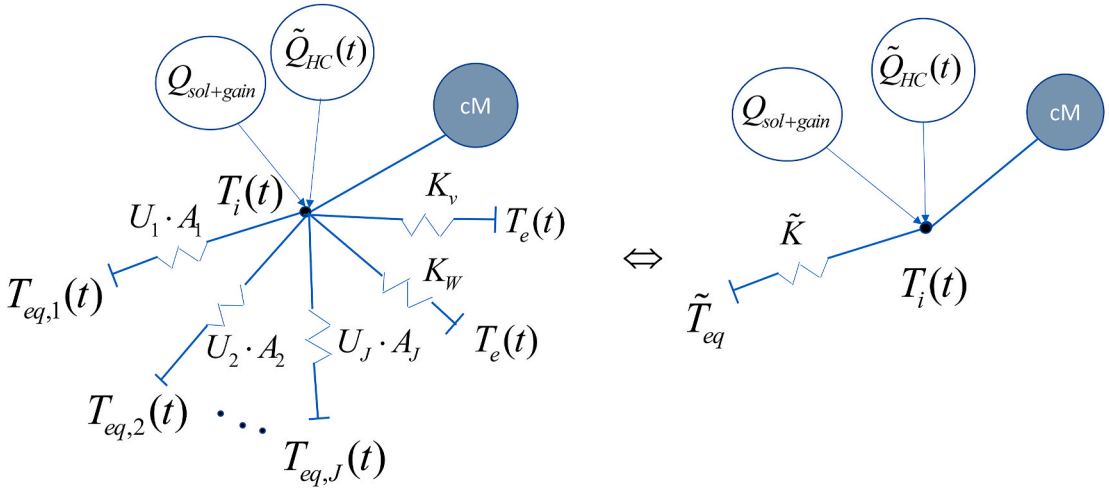

Fig. 5. Simplified networks representing the Conceptual model.

the character tilde (~).

The network in Fig. 5, left is transformed to a simpler one using network reduction, see Fig. 5, right. The total conductance $\tilde{K}$ (W/K[Btu/hr,°F]) between the exterior and the interior temperature is:

$$\tilde{K} = K_{wall} + K_W + K_v \tag{5}$$

where

$$K_{wall} = \sum_{j=1}^{J} U_j A_j \tag{6}$$

The equivalent boundary temperature, $\tilde{T}_{eq}$, defined by Eq. (7), accounts for the overall thermal coupling between the interior and the exterior. To account for ground heat losses, the boundary temperature can be represented by the annual average temperature of the location

and the U-value calculated by the ISO code [31]. However, this is not studied further in this article.

Fig. 6 shows the superposition of two networks that combined equal that of Fig. 5, right.

3.2. Defining building characteristics and the driving temperature

We denote $\tilde{T}_{eq}$ (K[°F]) the External Load Temperature (ELT).

$$\tilde{T}_{eq} = \frac{\sum_{j=1}^{J} U_j A_j \cdot T_{eq,j} + K_W \cdot T_e + K_v \cdot T_e}{\tilde{K}} \tag{7}$$

In Eq. (8), $\Delta\tilde{T}_{in}$(K[°F]) is a fictitious increase in external temperature that, when combined with the mutual building envelope conductance, $\tilde{K}$, results in an energy source corresponding to that of the solar load and internal heat gains. When $\Delta\tilde{T}_{in} > 0$ the heat flow towards the interior of the building increases and can result in higher cooling demand. If instead it is less than zero it can result in an increased heating demand during winter.

$$\Delta\tilde{T}_{in} = \frac{Q_{sol} + Q_{gain}}{\tilde{K}} \tag{8}$$

A *Thermal Load Resistance* (TLR), $\tilde{R}_{env}$(m^{2}K/W[hr,ft^2,°F/Btu]), which is an effective thermal resistance of the whole building envelope including the effect of air infiltration, will also be used. It is defined from the relations:

$$\tilde{R}_{env} = \frac{A_{env}}{\tilde{K}} \tag{9}$$

where

$$A_{env} = A_{wall} + A_W \tag{10}$$

$$A_{wall} = \sum_{j=1}^{J} A_j \tag{11}$$

$$A_W = \sum_{m=1}^{M_W} A_{W,m} \tag{12}$$

TLR reveals how impactful the exterior climate on the indoor climate is. It is also time-dependent since the infiltration rate changes over time.

Finally, an overall *Driving Temperature* (DT) is defined. This represents the overall climatic influence on the building in temperature degrees:

$$\tilde{T}_{DR} = \tilde{T}_{eq} + \Delta\tilde{T}_{in} \tag{13}$$

Fig. 7 shows the reduced final network representing the Conceptual model.

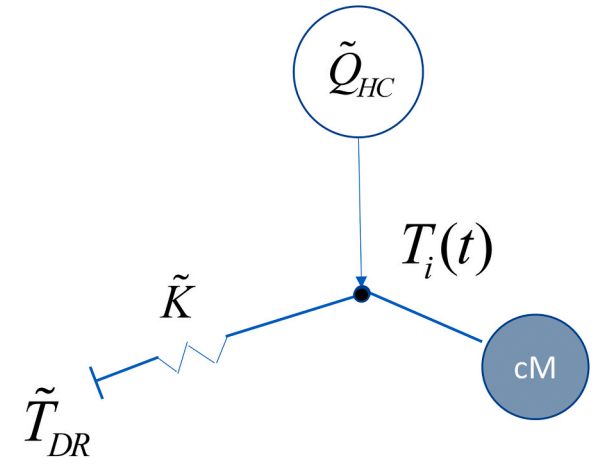

Fig. 7. Simplified network representing the Conceptual model of this paper. The driving temperature, $\tilde{T}_{DR}$, i.e. the sum of the External Load Temperature, and the internal Load Temperature is illustrated.

With this formulation, the heat flow to the interior becomes:

$$\tilde{K} \cdot \left(\tilde{T}_{DR} - T_i \right) \tag{14}$$

In the following paragraphs of this paper, the effect of the building design and the coupling to the climate is of interest. Therefore, any internal heat gains, Q_{gain}, other than that of solar gains Q_{sol}, will not be accounted for in $\tilde{T}_{DR}$.

The thermal mass can moderate variations in the interior temperature generated by the driving temperature. The free running temperature, T_{free} is defined as the interior temperature when neither heating nor cooling takes place, i.e. $\tilde{Q}_{HC} = 0$.

On the contrary, if the free running temperature is outside the thermostat setpoint range, heating or cooling is needed during this time. Using $\tilde{Q}_{HC}$, an additional driving temperature can be expressed in the network as $\Delta\tilde{T}_{HC}$.

$$\Delta\tilde{T}_{HC} = \frac{\tilde{Q}_{HC}}{\tilde{K}} \tag{15}$$

With this last step we have reduced the thermal problem to a simple dynamic model for a lumped system. There is a driving effective boundary temperature, a coupling to the interior temperature T_i by one conductance, and a lumped mass representing all thermal mass of the

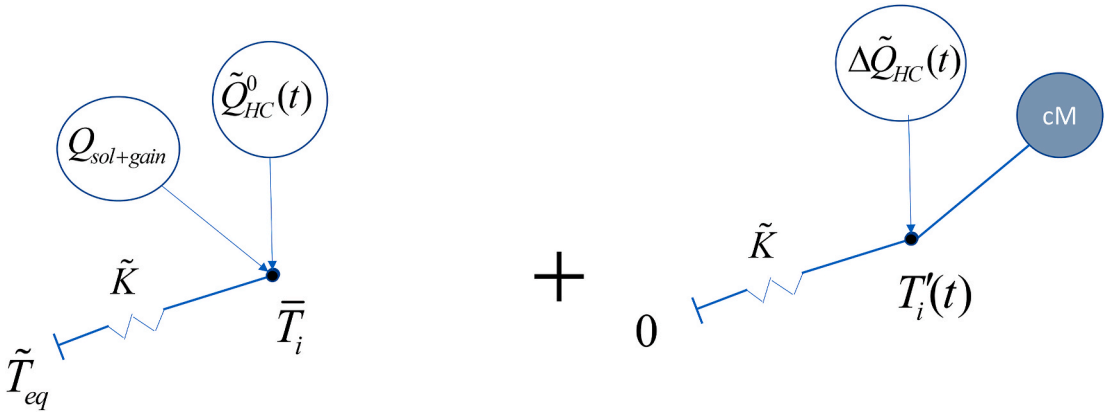

Fig. 6. The Conceptual network model divided into two networks using superposition.

interior. See Fig. 8.

The free running temperature is obtained from

$$\tilde{T}_{DR} - T_{free} = t_c \frac{dT_{free}}{dt} \tag{16}$$

with

$$t_c = \frac{cM}{\tilde{K}} \tag{17}$$

The changes in temperature, $\tilde{T}_{HC}$, due to the heating and cooling effect contained in $\Delta\tilde{T}_{HC}$ becomes:

$$\Delta\tilde{T}_{HC} - \tilde{T}_{HC} = t_c \frac{d\tilde{T}_{HC}}{dt} \tag{18}$$

The $\Delta\tilde{T}_{HC}$ is chosen so that resulting indoor temperature, equal to $T_{free} + \tilde{T}_{HC}$, satisfies:

$$\overline{T}_i - \frac{\Delta T}{2} \le \left(T_{free}(t) + \tilde{T}_{HC}(t)\right) \le \overline{T}_i + \frac{\Delta T}{2} \tag{19}$$

The presented solution technique below uses the free running temperature from time step to time step with an assumed fixed value of $\Delta\tilde{T}_{HC}$, for each time step to be calculated if required.

3.3. Solution techniques

A numerical algorithm is briefly given here for solving Eq.'s (16) through (19). With a given temperature at the previous time step t_{n-1}, without any heating or cooling i.e.$\Delta\tilde{T}_{HC,n} = 0$, the free running temperature after one time step becomes:

$$T_i^0(t_n) = T_i(t_{n-1}) + \left(\tilde{T}_{DR,n} - T_i(t_{n-1})\right) \cdot \left(1 - e^{-\Delta t/t_{c,n}}\right) \quad \Delta t = t_n - t_{n-1} \tag{20}$$

The formula shows that the indoor temperature reaches $\tilde{T}_{DR,n}$ after longer times, since the exponential term will then vanish. If $T_i^0(t_n)$ is within the comfort span neither heating nor cooling is needed and the temperature at time t_n , i.e. $T_i(t_n)$ is determined by $T_i^0(t_n)$. If this is not the case, heating or cooling is required to maintain $T_i(t_n)$ within the thermostat setpoint temperatures.

For cooling demand

$$T_i^0(t_n) > \overline{T}_i + \frac{\Delta T}{2} \Rightarrow \Delta\tilde{T}_{HC,n} = -\frac{T_i^0(t_n) - \left(\overline{T}_i + \frac{\Delta T}{2}\right)}{1 - e^{-\Delta t/t_{c,n}}} \Rightarrow T_i(t_n) = \overline{T}_i + \frac{\Delta T}{2} \tag{21}$$

And heating:

$$T_i^0(t_n) < \overline{T}_i - \frac{\Delta T}{2} \Rightarrow \Delta\tilde{T}_{HC,n} = \frac{\left(\overline{T}_i - \frac{\Delta T}{2}\right) - T_i^0(t_n)}{1 - e^{-\Delta t/t_{c,n}}} \Rightarrow T_i(t_n) = \overline{T}_i - \frac{\Delta T}{2} \tag{22}$$

The algorithm tells us that when heating is required, temperature it is locked to $\overline{T}_i - \frac{\Delta T}{2}$. When cooling is required the temperature is locked to $\overline{T}_i + \frac{\Delta T}{2}$. If neither is required, the free running temperature is used with an initial value from the previous timestep.

The required heating or cooling during the time step, $\tilde{Q}_{HC,n}$, is then obtained through (15). This procedure is stable for any time step since analytical exponential solutions are used that are bounded by the given heating or cooling load.

3.4. Accuracy

An assumption made for the conceptual model is that a single temperature is representative for that of the interior space, and no distinction is made for convective and radiative heat exchange. The accuracy of the conceptual model is also coupled to the assumption that temperatures of the inner most material layer is following the interior temperature. A main driver for interior temperature variations is diurnal variations. For thick material layers, it is less accurate to assume that the surface temperature will propagate into the material and thus activate the whole thermal mass. As a control mechanism, the conceptual model of this paper relies on a criterion, in which an upper thickness $d_{\max,j}$ (m [ft]) for inner surface layers j must be satisfied. Using [32], the following criterion must be met:

$$d_{\max,j} \le 0.75 \cdot d_{p,j} \tag{23}$$

$$d_{p,j} = \sqrt{\frac{a_j \cdot t_p}{\pi}} \quad j = 1 \ldots J \tag{24}$$

Here, a_j(m^2/s[ft^2/s]) is the thermal diffusivity of the inner material layer and t_p(s) is the time period i.e. 24 h.

As an example, the penetration depth d_p(m[ft]) for a diurnal variation in concrete is a round 0.15 m and for gypsum it is around 0.09 m. The criteria (23) is found as the limit when the heat storage in a lump and in a layer with an adiabatic (insulated) back side both are exposed at its surface with a sinusoidal temperature variation differs with less than 9.3%. (for a limit equal to d_p the error is 26.6%).

Four building cases are analyzed and present in the Appendix of this paper. These cases show that there is close match between the conceptual model and the more sophisticated one as seen in Fig. 2. The four cases are a combination of light and heavy walls and floors. The error between the models for step changes in the external equivalent temperature is less than 20% for the transmission through the layered walls. The error due to a response in the internal temperature due to internal gain changes are 0.7–11.7%. However, the overall impact on the energy

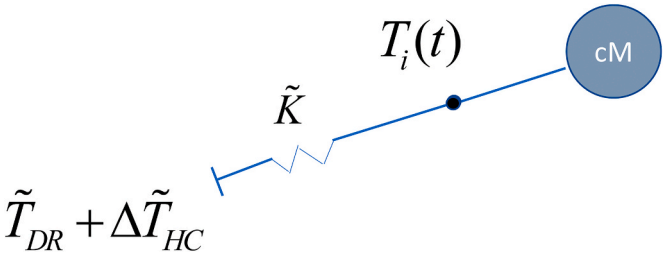

Fig. 8. Fully simplified network represented by one boundary temperature and one lump. The boundary temperature for the node is the sum of the driving temperature in Eq. (13) and the added heating and cooling effect temperature in Eq. (15).

demand over longer period is limited for the shown synthetic climate data year case. As an estimate the conceptual model gives an error for the dominating cooling demand of only 3%. For the much smaller heating demand the error is between 3 and 22%.

The conceptual model is used to calculate the energy demand and a cooling proportion indicator that are mapped for a whole country or region. For a specific building, with a given building envelope, we can expect the error in the calculated indicators be similar and the comparisons to be adequate.

4. Building envelope and driving temperature characteristics for buildings across the U.S. using the conceptual model

The main goal with the analysis is to find patterns that make it possible, from known building and climate data, to estimate the total yearly energy demand E (J[Btu]), and the ratio between heating and cooling.

$$\begin{cases} E_{cooling+heating} = \int_0^{t_{year}} \left|\tilde{Q}_{HC}\right| dt \\ E_{cooling} = \beta \cdot E_{cooling+heating} \\ E_{heating} = (1-\beta) \cdot E_{cooling+heating} \end{cases} \tag{25}$$

Here, t_{year}(s) is the time length of one year. The last formula in Eq. (25) introduces $\beta(-)$, which represents the ratio of cooling over the overall heating and cooling energy demand.

The following total energy demand gives the base line (maximum required energy), i.e. with a strict control of the interior temperature, with $\Delta T = 0$, meaning also that thermal mass storage is not dynamically used:

$$E^0_{cooling+heating} = \int_0^{t_{year}} \left|\tilde{Q}^0_{HC}\right| dt = \tilde{K} \cdot \int_0^{t_{year}} \left|\tilde{T}_{DR} - \overline{T}_i\right| dt = \tilde{K} \cdot \overline{\left|\tilde{T}_{DR} - \overline{T}_i\right|} \cdot t_{year} \quad \Delta T = 0 \tag{26}$$

The Building Envelope Performance (BEP) value (J/m^2[Btu/ft^2]) is introduced in [26] and represent the overall energy demand due to building envelope related thermal loads over the whole building envelope surface area.

$$BEP = \frac{E_{cooling+heating}}{A_{env}} \tag{27}$$

$$BEP^0 = \frac{E^0_{cooling+heating}}{A_{env}} \tag{28}$$

$$\alpha = \frac{BEP}{BEP^0} \tag{29}$$

The second variable, BEP^0, can be calculated using the climate and the building construction data only. Again, "0" represents the base case for which the indoor temperature is remained fixed and thus maximum heating and cooling demand. Using BEP, the parameter α, which is in the range between zero and one, represents the ratio of the BEP-value between the base case and the case for which the indoor temperature is allowed to float within the thermostat setpoints.

Further, we introduce the Driving Temperature Difference (DTD), $\Delta\tilde{T}_{TD}$(K[°F]) as the annual average and absolute difference between the average indoor temperature and the driving temperature:

$$\Delta\tilde{T}_{TD} = \overline{\left|\tilde{T}_{DR} - \overline{T}_i\right|} \tag{30}$$

$$BEP^0 = \Delta\tilde{T}_{TD} \cdot \frac{\tilde{K} \cdot t_{year}}{A_{env}} = \frac{\Delta\tilde{T}_{TD}}{\tilde{R}_{env}} t_{year} \tag{31}$$

$$BEP^0 = \frac{\Delta\tilde{T}_{TD}}{\tilde{R}_{env}} \cdot 8.76 \quad \text{kWh/m}^2 \tag{32}$$

DTD is determined by present climate conditions, solar absorptivity and long wave emissivity's of the external surfaces, together with the convective heat transfer, U-values, areas, air infiltration rate and solar gains through the windows. Hence, DTD is a building and climate data specific value.

To get information of the fraction of heating and cooling we will utilize β, which is in the range between zero and one:

$$BEP^C = \beta \cdot BEP \tag{33}$$

$$BEP^H = (1-\beta) \cdot BEP \tag{34}$$

The two ratios α and β are obtained from simulations accounting for climate data, the mid setpoint temperature $\overline{T}_i$, the thermal comfort interval ΔT, the overall thermal conductance $\tilde{K}$, and the thermal mass cM. With this information given, the time constant is defined in relation to the time period of the day:

$$t_c \,/\, t_p = \frac{cM}{\tilde{K} \cdot t_p} = \frac{(cM/A_{env}) \cdot \tilde{R}_{env}}{t_p} \tag{35}$$

$$t_c = \frac{cM}{A_{env}} \tilde{R}_{env} \tag{36}$$

The time constant t_c[s] is here formulated as the thermal mass cM (J/K[Btu/°F]) per building envelope unit area unit, multiplied with the thermal load resistance $\tilde{R}_{env}$(m^{2}K/W[hr,ft^2,°F/Btu]).

Fig. 9 presents the different climate zones across the U.S. used in this study. Table 1 shows how the introduced metrics vary using various climate and building data [28], using a "Medium Office" building. The upper and lower thermostat setpoint are set to 24 and 22 °C [71.6 to 75.2 °F]. Here, the office building has different envelope characteristics depending on location and building code. The term $\overline{\tilde{T}_{DR}}$ is the annual average driving temperature, and $\overline{\tilde{T}_{DR,A,day}}$ is the average 24-hours amplitude, defined as half the difference between the maximum and minimum driving temperature during a 24 h period. The corresponding amplitude for the year $\overline{\tilde{T}_{DR,A,year}}$ is based on moving monthly mean values.

We can observe significantly low α value of 0.66 for climate zone 3C, i.e. San Francisco region in California. This means that the free running temperature more frequently stays within the comfort interval, thus the temperature control system will not call for heating or cooling as often. In this climate, the cooling is only 6% of the total energy demand, i.e. mainly heating required.

The following example shows how the table values can be used.

Examples (SI-units):

Climate zone 4A. Using Eq. (30)-(32).

$$BEP^0 = \frac{\Delta\tilde{T}_{TD}}{\tilde{R}_{env}} \cdot 8.76 = \frac{11.77}{0.63} \cdot 8.76 = 163.6 \ \text{kWh/m}^2$$

$$BEP = \alpha \cdot BEP^0 = 0.78 \cdot 163.6 = 127.7 \ \text{kWh/m}^2$$

Since is $\beta = 0.19$, 19% of the total energy demand is from cooling, i.e. 24.5 kWh/m^2.

Fig. 10 through 12 map $\alpha\,(-), \beta\ (-)$ and $\Delta\tilde{T}_{TD}$(K) across the U.S. for a building complying with EnergyPlus climate zone '3A' (Atlanta, Georgia), Medium Office (see Fig. 23), $\overline{T}_i = 23$°C, $\Delta T = 2$°C and $t_c/t_p = 1.044\ (0.0636)$, $\tilde{R}_{env} = 0.5425\ (0.0330)$m^{2}K/W. The values represent the mean and standard deviation (in parenthesis). These variations are a result varying air infiltration rates caused by stack effect and wind loads. The annual average air infiltration rate is used in the conceptual model analysis. The driving temperature difference $\Delta\tilde{T}_{TD}$ range from 8 °C in

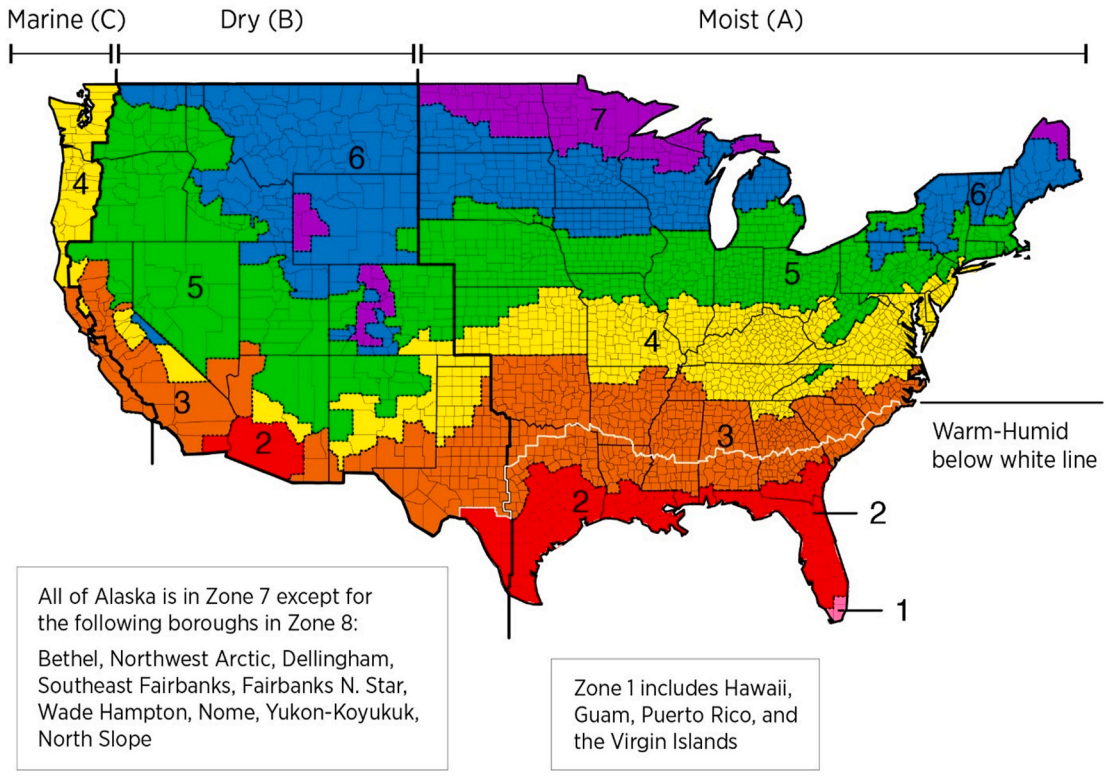

Fig. 9. U.S. Climate zones [33].

Table 1
Results for EnergyPlus climatic and building data, Medium Office with building specification dependent on location and local building code. Values are displayed in SI units. The table includes values for the Driving Temperature Difference (DTD), $\Delta\tilde{T}_{TD}$, α and β values, the time constant, t_c/t_p,the overall building envelope thermal conductance and thermal load resistance, $\tilde{K}$ and $\tilde{R}_{env}$, as well as the average outdoor air temperature for the location, $\overline{T}_e$. The term $\overline{\tilde{T}_{DR}}$ is the annual average driving temperature, and $\overline{\tilde{T}_{DR,A,day}}$ is the average 24-hours amplitude, defined as half the difference between the maximum and minimum driving temperature during a 24 h period. The corresponding amplitude for the year $\overline{\tilde{T}_{DR,A,year}}$ is based on moving monthly mean values.

Climate Zone	$\Delta\tilde{T}_{TD}(^{\circ}C)$	$\alpha(-)$	$\beta(-)$	$t_c/t_p(-)$	$\tilde{K}$(kW/K)	$\tilde{R}_{env}$(m^{2}K/W)	$\overline{T}_e(^{\circ}C)$	$\overline{\tilde{T}_{DR}}(^{\circ}C)$	$\overline{\tilde{T}_{DR,A,day}}(^{\circ}C)$	$\overline{\tilde{T}_{DR,A,year}}(^{\circ}C)$
1A	5.82	0.72	0.85	0.66	10.55	0.34	24.51	26.54	8.03	5.1
2A	7.17	0.70	0.51	0.93	7.51	0.48	21.08	23.21	8.05	8.2
2B	10.05	0.78	0.68	0.89	7.88	0.46	23.80	26.09	10.39	12.3
3A	9.51	0.74	0.25	1.06	6.58	0.55	16.65	19.26	8.48	12.2
3B	10.33	0.80	0.43	0.88	7.97	0.46	19.84	21.78	9.06	13.5
3C	9.06	0.66	0.06	0.98	7.12	0.51	13.79	17.21	9.19	4.7
4A	11.77	0.78	0.19	1.22	5.76	0.63	13.21	16.90	10.12	14.2
4B	11.77	0.74	0.21	1.10	6.39	0.57	13.68	17.61	14.38	12.5
4C	11.55	0.78	0.05	1.11	6.33	0.57	11.24	14.24	7.09	9.2
5A	14.14	0.83	0.12	1.17	5.99	0.61	9.99	13.66	10.74	16.2
5B	14.04	0.76	0.12	1.22	5.72	0.64	10.30	14.38	13.11	13.6
6A	15.85	0.84	0.10	1.24	5.63	0.65	7.73	11.74	9.64	19.2
6B	15.77	0.82	0.07	1.29	5.42	0.67	7.16	11.36	12.52	15.1
7A	17.81	0.85	0.06	1.24	5.66	0.64	4.02	8.92	9.46	18.0
8A	24.05	0.88	0.05	1.36	5.16	0.71	−1.43	3.38	4.32	24.8

Florida to 18 °C in the Northern states. The α parameter varies between 0.6 in the coastal areas of California to 0.9 in Minnesota. The value is rather flat between 0.7 and 0.85 in main parts of the remaining states. The β value, which is a fraction of cooling on the overall energy demand, ranges from around 0 in the Northern states to 0.9 in Southern Florida.

Fig. 13 through Fig. 15 map $\alpha\,(-), \beta\,(-)$ and $\Delta\tilde{T}_{TD}$(K) across the U.S. for a building complying with EnergyPlus climate zone '7A' (Atlanta, Georgia), Medium Office, $\overline{T}_i = 23^{\circ}C$, $\Delta T = 2^{\circ}C$ and $t_c/\ t_p = 1.3696\ (0.1082)$,$\tilde{R}_{env} = 0.7116\ (0.0562)$ m^{2}K/W. Compared to previous building in '3A', a climate zone '7A' "Medium Office" building has higher R-value requirements. The driving temperature difference $\Delta\tilde{T}_{TD}$ range from 10 °C in Florida to 18 (°C) in the Northern states. The α parameter varies between 0.5 in the coastal areas of California to 0.85 in the Northern states. The value is rather flat between 0.65 and 0.85 in main parts of the remaining states. The β value ranges from around 0.1 in the Northern states to 0.9 in Florida.

Table 2 through Table 5 provide the results for a "Medium office" building based on climate zone 3A energy code requirements and located in four climate locations. The analyses are made for doubled indoor temperature comfort interval range, and an internal thermal mass multiplied with 2,4 and 0.5 respectively. The locations are (3A) Athens, Georgia (humid subtropical), (3B) Las Vegas, Nevada, subtropical desert climate, (4A) Baltimore, Maryland (in the Mid-Atlantic

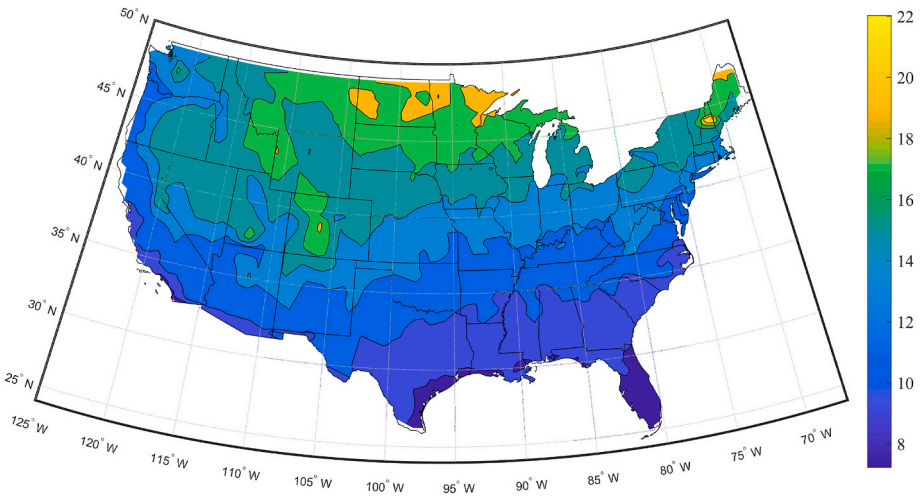

Fig. 10. $\Delta \tilde{T}_{TD}(^{\circ}C)$ for a prescribed Climate Zone 3A "Medium Office" building across the U.S.

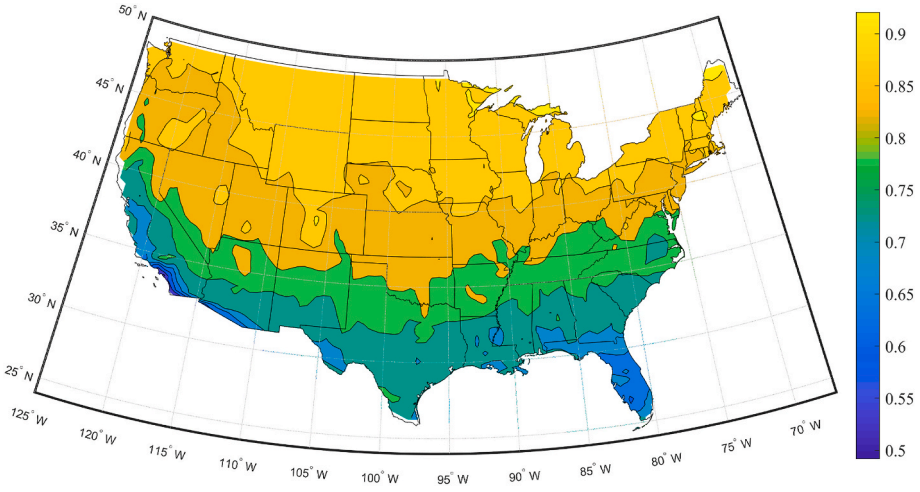

Fig. 11. α for a prescribed Climate Zone 3A "Medium Office" building across the U.S.

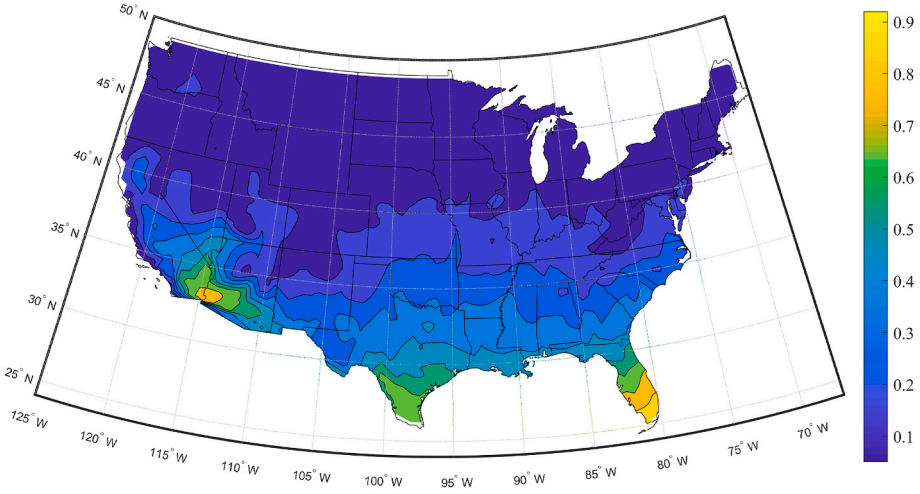

Fig. 12. β for a prescribed Climate Zone 3A "Medium Office" building across the U.S.

region of the eastern) and (7A) Duluth, Minnesota (Upper Midwest, Great Lakes, and northern regions). The tables show that increasing the thermal mass and widening the acceptable temperature range results in a 9 to 24% lower energy demand. The greatest reduction is found in (3A) Athens, Georgia.

Fig. 16 through Fig. 18 map $\alpha\ (-), \beta\ (-)$ and $\Delta \tilde{T}_{TD}$across the U.S. for

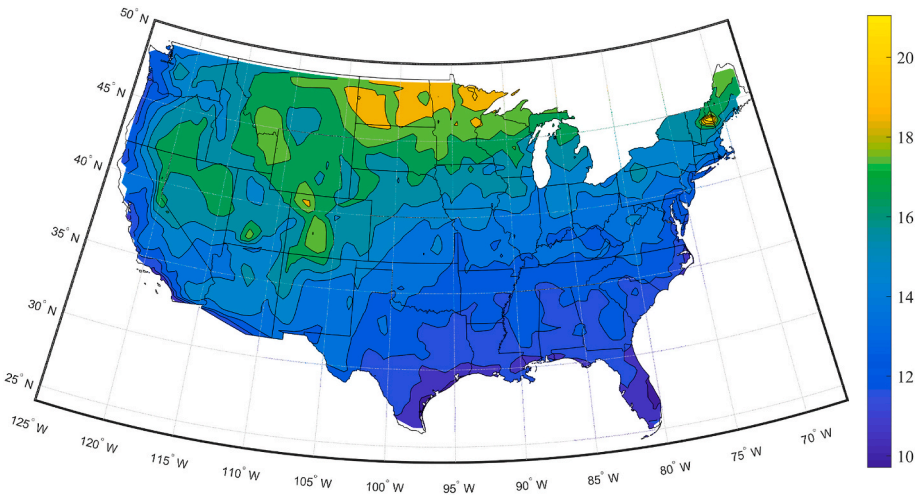

Fig. 13. $\Delta \tilde{T}_{TD}(^{\circ}C)$ for a prescribed Climate Zone 7A "Medium Office" building across the U.S.

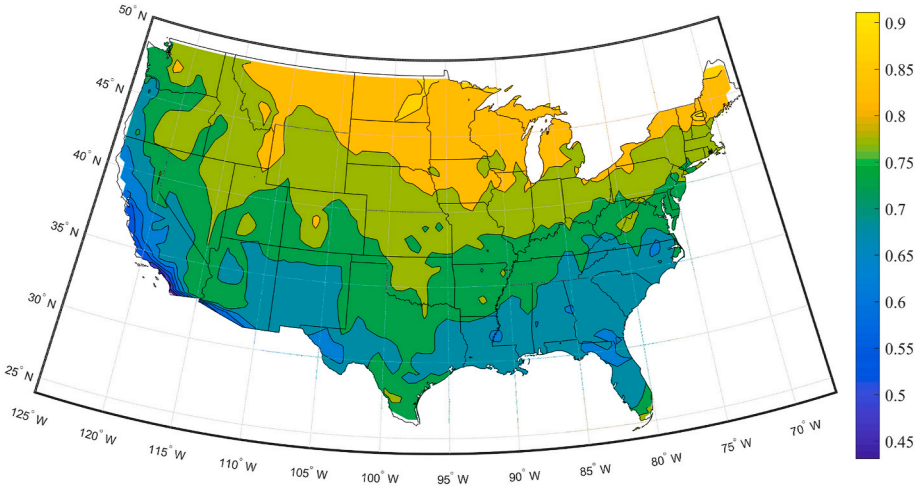

Fig. 14. -α for a prescribed Climate Zone 7A "Medium Office" building across the U.S.

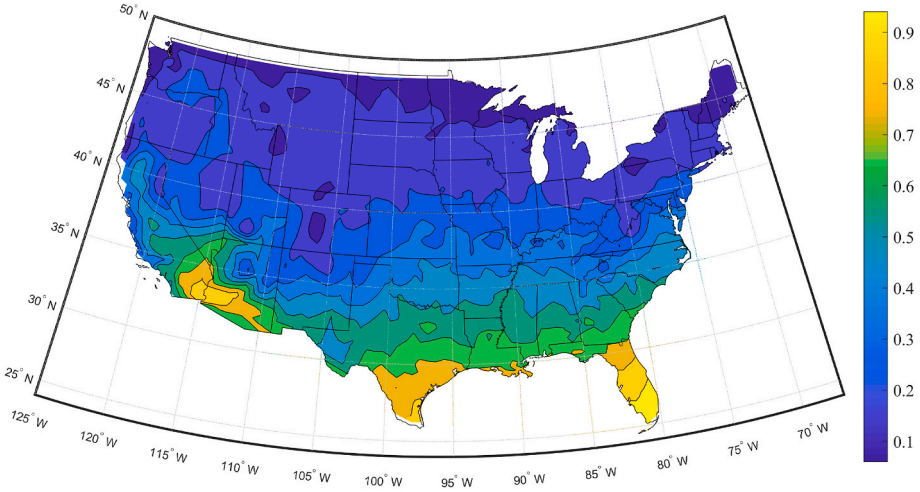

Fig. 15. β for a prescribed Climate Zone 7A "Medium Office" building across the U.S.

a building complying with EnergyPlus climate zone '3B' (Las Vegas, Nevada), Large Hotel, $\overline{T}_i = 23^{\circ}C$, $\Delta T = 2^{\circ}C$ and $t_c/t_p = 0.805\ (0.036)$,$\tilde{R}_{env} = 0.336\ (0.015)\ m^2K/W$.

The driving temperature difference $\Delta \tilde{T}_{TD}$ranges from 8 °C in Florida to 18 °C in the Northern states. The αparameter varies between 0.55 in the coastal areas of California to 0.9 in the Northern states. The value is

Table 2
The parameters $\alpha(-), \beta(-)$ for climate zone '3A', Medium Office located in Athens, Georgia, $\overline{T}_i = 23(^{\circ}C)$, for varying comfort interval and thermal mass, with building envelope characteristics of $\tilde{R}_{env} = 0.58 m^2K/W$, $BEP^0 = 140.2 kWh/m^2$, and $\Delta\tilde{T}_{TD} = 9.3^{\circ}C$.

	$\Delta T = 2$ °C	$\Delta T = 4$ °C	$\Delta T = 2$ °C	$\Delta T = 2$ °C	$\Delta T = 2$ °C
	$t_c/t_p = 1.12$	$t_c/t_p = 1.12$	$t_c/t_p = 2.24$	$t_c/t_p = 4.48$	$t_c/t_p = 0.56$
α	0.722	0.601	0.675	0.654	0.789
β	0.236	0.200	0.217	0.210	0.261

Table 3
The parameters $\alpha(-), \beta(-)$ for climate zone '3A', Medium Office located in Las Vegas, Nevada, $\overline{T}_i = 23^{\circ}C$, for varying comfort interval and thermal mass, with building envelope characteristics of $\tilde{R}_{env} = 0.53 m^2K/W$, $BEP^0 = 174.6 kWh/m^2$, and $\Delta\tilde{T}_{TD} = 10.6^{\circ}C$.

	$\Delta T = 2$ °C	$\Delta T = 4$ °C	$\Delta T = 2$ °C	$\Delta T = 2$ °C	$\Delta T = 2$ °C
	$t_c/t_p = 1.03$	$t_c/t_p = 1.03$	$t_c/t_p = 2.05$	$t_c/t_p = 4.10$	$t_c/t_p = 0.51$
α	0.787	0.683	0.757	0.742	0.833
β	0.456	0.453	0.455	0.456	0.458

Table 4
The parameters $\alpha(-), \beta(-)$ for climate zone '3A', Medium Office located in Baltimore, Maryland, $\overline{T}_i = 23^{\circ}C$, for varying comfort interval and thermal mass, with building envelope characteristics of $\tilde{R}_{env} = 0.51 m^2K/W$, $BEP^0 = 219.1 kWh/m^2$, and $\Delta\tilde{T}_{TD} = 12.9^{\circ}C$.

	$\Delta T = 2$ °C	$\Delta T = 4$ °C	$\Delta T = 2$ °C	$\Delta T = 2$ °C	$\Delta T = 2$ °C
	$t_c/t_p = 0.99$	$t_c/t_p = 0.99$	$t_c/t_p = 1.98$	$t_c/t_p = 3.96$	$t_c/t_p = 0.50$
α	0.865	0.782	0.845	0.837	0.889
β	0.043	0.028	0.033	0.028	0.055

Table 5
The parameters $\alpha(-), \beta(-)$ for climate zone '3A', Medium Office located in Duluth, Minnesota, $\overline{T}_i = 23^{\circ}C$, for varying comfort interval and thermal mass, with building envelope characteristics of $\tilde{R}_{env} = 0.53 m^2K/W$, $BEP^0 = 310.7 kWh/m^2$, and $\Delta\tilde{T}_{TD} = 18.9^{\circ}C$.

	$\Delta T = 2$ °C	$\Delta T = 4$ °C	$\Delta T = 2$ °C	$\Delta T = 2$ °C	$\Delta T = 2$ °C
	$t_c/t_p = 1.03$	$t_c/t_p = 1.03$	$t_c/t_p = 2.05$	$t_c/t_p = 4.10$	$t_c/t_p = 0.51$
α	0.901	0.836	0.879	0.868	0.922
β	0.023	0.011	0.012	0.007	0.033

rather flat between 0.75 and 0.85 in main parts of the remaining states. The βvalue ranges from around 0 in the Northern states, about 0.1 in the coastal regions of California, to 0.9 in Southern Florida.

Fig. 19 through Fig. 21 map $\alpha(-), \beta(-)$ and $\Delta\tilde{T}_{TD}$ across the U.S. for a building complying with EnergyPlus climate zone '4A' (Baltimore, Maryland), Large Hotel, $\overline{T}_i = 23^{\circ}C$, $\Delta T = 2^{\circ}C$ and $t_c/t_p = 1.221\ (0.082)$, $\tilde{R}_{env} = 0.510\ (0.034)\ m^2K/W$.

The driving temperature difference $\Delta\tilde{T}_{TD}$ range from 8 °C in Florida to 18 °C in the Northern states. The αparameter varies between 0.5 in the coastal areas of California to 0.7 in the Northern states. The value is rather flat between 0.7 and 0.8 in the main parts of the remaining states. The β value ranges from around 0 in the Northern states to 0.9 down in Florida.

5. Design process using the conceptual model

Fig. 22 illustrates the tasks and information needed by the Conceptual model. It also shows different climate and building characteristics that the model displays. The right-hand part of the figure reveals various thermal performance metric options for overall energy and peak demand calculations.

Example (SI-units):

Let us study the Medium Office in climate zone 3A (Athens, Georgia). The data form [28]. Total floor area 4980 m^2. (Bottom floor heat loss neglected).

$\overline{T}_i = 23^{\circ}C$, $\Delta T = 2^{\circ}C$ $t_c/t_p = 1.12$, $\tilde{R}_{env} = 0.582\ m^2K$ $\Delta K = 6252 W/K$

$A_w = 652.8\ m^2$ $A_{wall} = 1\ 325\ m^2$ $A_{roof} = 1\ 660\ m^2$ $cM = 6.05 \cdot 10^8\ J/K$.

$U_w = 4.10 W/m^2K$ $U_{wall} = 0.730 W/m^2K$ $U_{roof} = 0.414 W/m^2K$ $R_a = 1.60\ m^3/s$

$g = SHGC = 0.255$.

Fig. 24 shows the calculated heating and cooling demand during the year. Based on the algorithm in subsection 3.3. We get:

$\Delta\tilde{T}_{TD} = 9.32^{\circ}C, \alpha = 0.722, \beta = 0.236$

$$BEP^0 = \frac{\Delta\tilde{T}_{TD}}{\tilde{R}_{env}} \cdot 8.76 = \frac{9.32}{0.582} \cdot 8.76 = 140.2\ kWh/m^2$$

$$BEP = \alpha \cdot BEP^0 = 0.722 \cdot 140.2 = 101.2\ kWh/m^2$$

$$BEP^C = \beta \cdot BEP = 0.236 \cdot 101.2 = 23.9\ kWh/m^2$$

The peak loads are 206 kW for heating, and 128 kW for cooling.

We test a changed thermal comfort interval.

$\Delta T = 6^{\circ}C$.

This gives:

$\alpha = 0.5135, \beta = 0.1725$

$$BEP = 0.5135 \cdot 140.2 = 72.0\ kWh/m^2$$

$$BEP^C = \beta \cdot BEP = 0.1725 \cdot 72 = 12.4\ kWh/m^2$$

For this case, the peak loads are 193 kW for heating, 115 kW for cooling.

This means that an increase in the comfort interval, ΔT, from 2 to 6 °C results in a reduction of the overall energy demand by 29% and the cooling demand decrease with 48%.

If, in addition to an increased ΔT, a 30% increase in R-values is assumed (same solar gains) and an improved airtightness by 20%, thus a lesser air flow rate, the following is given:

$\Delta\tilde{T}_{TD} = 9.72^{\circ}C$ $t_c/t_p = 1.533, \tilde{R}_{env} = 0.796\ m^2K/W$.

$\alpha = 0.4733, \beta = 0.2284$

$$BEP^0 = \frac{\Delta\tilde{T}_{TD}}{\tilde{R}_{env}} \cdot 8.76 = \frac{9.72}{0.796} \cdot 8.76 = 106.95\ kWh/m^2$$

$$BEP = \alpha \cdot BEP^0 = 0.4733 \cdot 106.94 = 50.6\ kWh/m^2$$

$$BEP^C = \beta \cdot BEP = 0.2284 \cdot 50.6 = 11.6\ kWh/m^2$$

The peak loads are 141 kW for heating and 95 kW for cooling.

The overall energy demand decreased further 30%, while the cooling demand changed by 6%.

Let us reduce the solar gains with 30% (decreased SHGC):

$\Delta\tilde{T}_{TD} = 9.24^{\circ}C$ $\alpha = 0.5052, \beta = 0.1564$

$$BEP^0 = \frac{\Delta\tilde{T}_{TD}}{\tilde{R}_{env}} \cdot 8.76 = \frac{9.24}{0.796} \cdot 8.76 = 101.7\ kWh/m^2$$

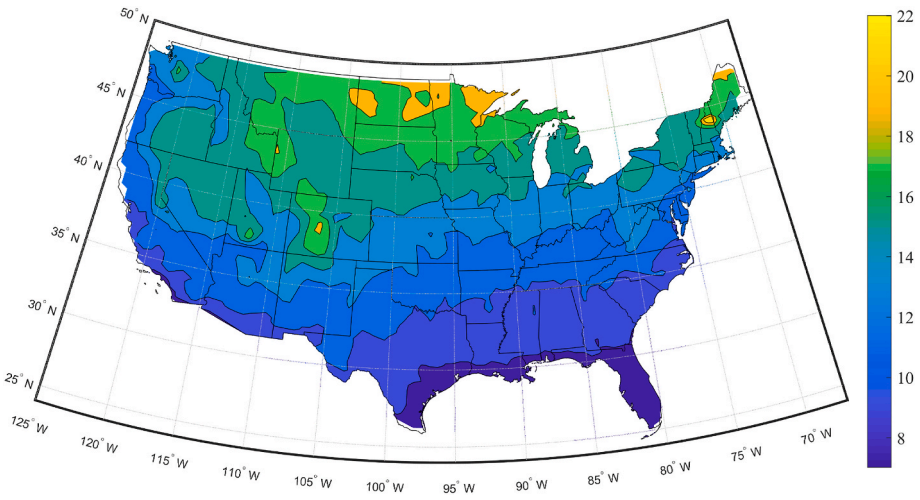

Fig. 16. $\Delta \tilde{T}_{TD}(^{\circ}C)$ for a prescribed Climate Zone 3B "Large Hotel' building across the U.S.

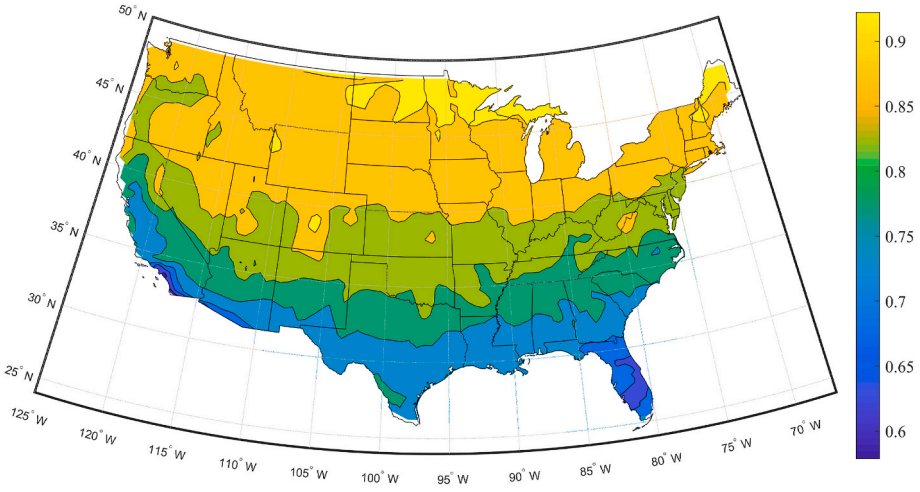

Fig. 17. α for a prescribed Climate Zone 3B "Large Hotel" building across the U.S.

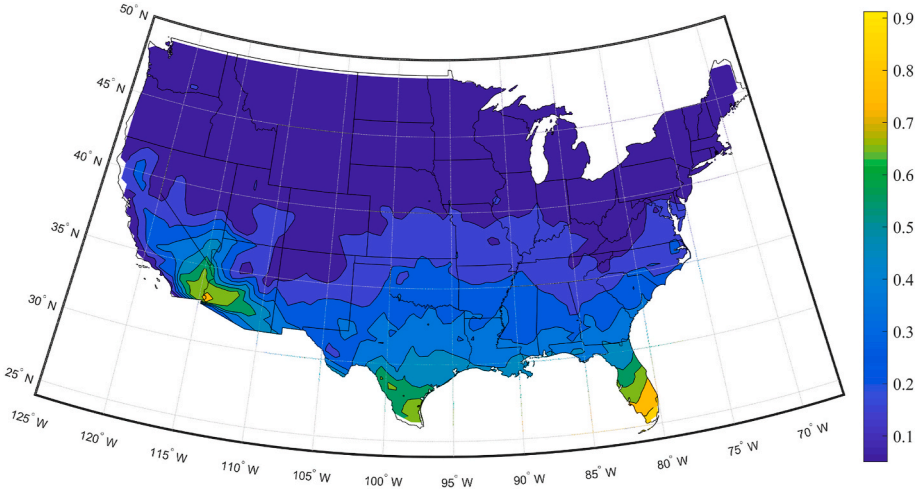

Fig. 18. β for a prescribed Climate Zone 3B "Large Hotel" building across the U.S.

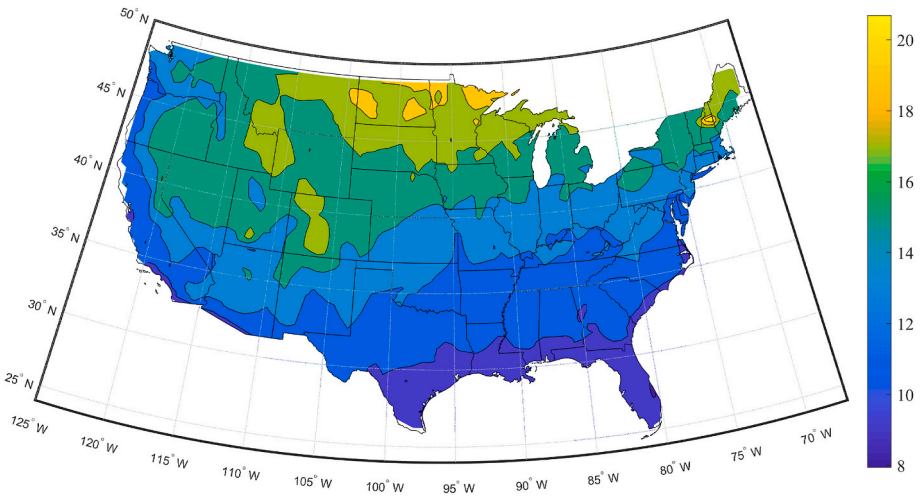

Fig. 19. $\Delta \tilde{T}_{TD}(^{\circ}C)$ for a prescribed Climate Zone 4A "Large Hotel' building across the U.S.

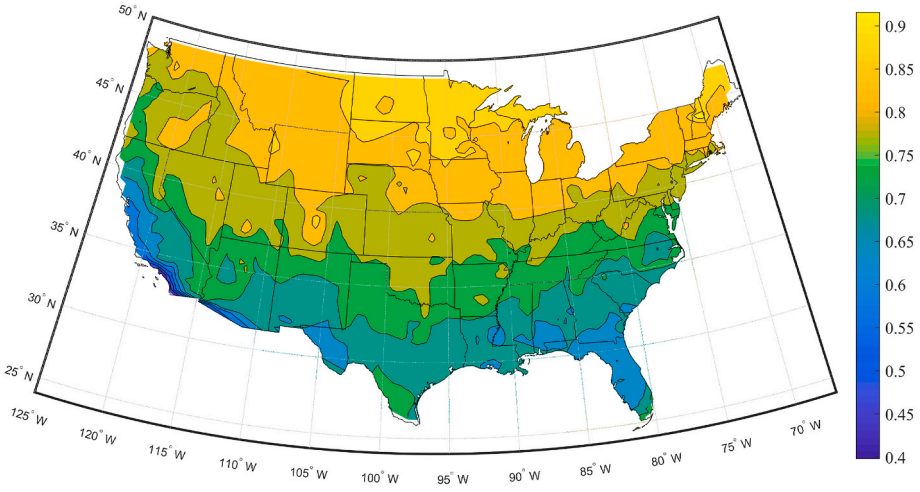

Fig. 20. α for a prescribed Climate Zone 4A "Large Hotel' building across the U.S.

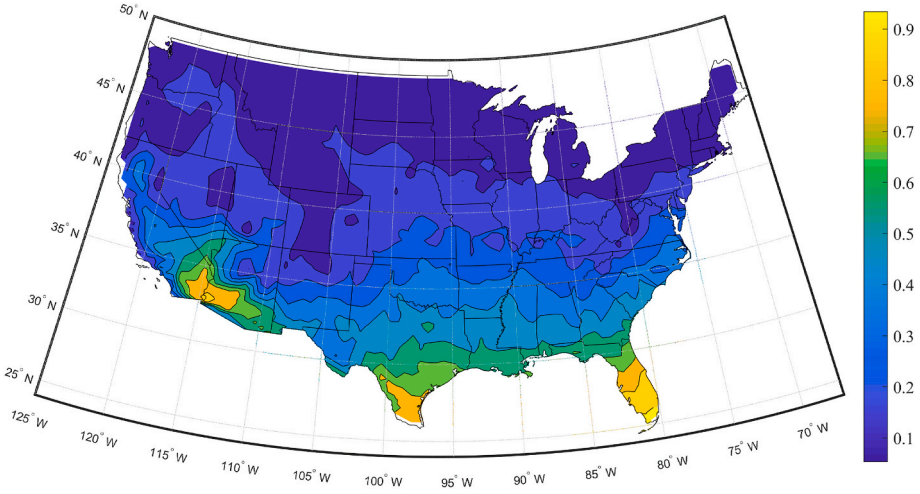

Fig. 21. β for a prescribed Climate Zone 4A "Large Hotel" building across the U.S.

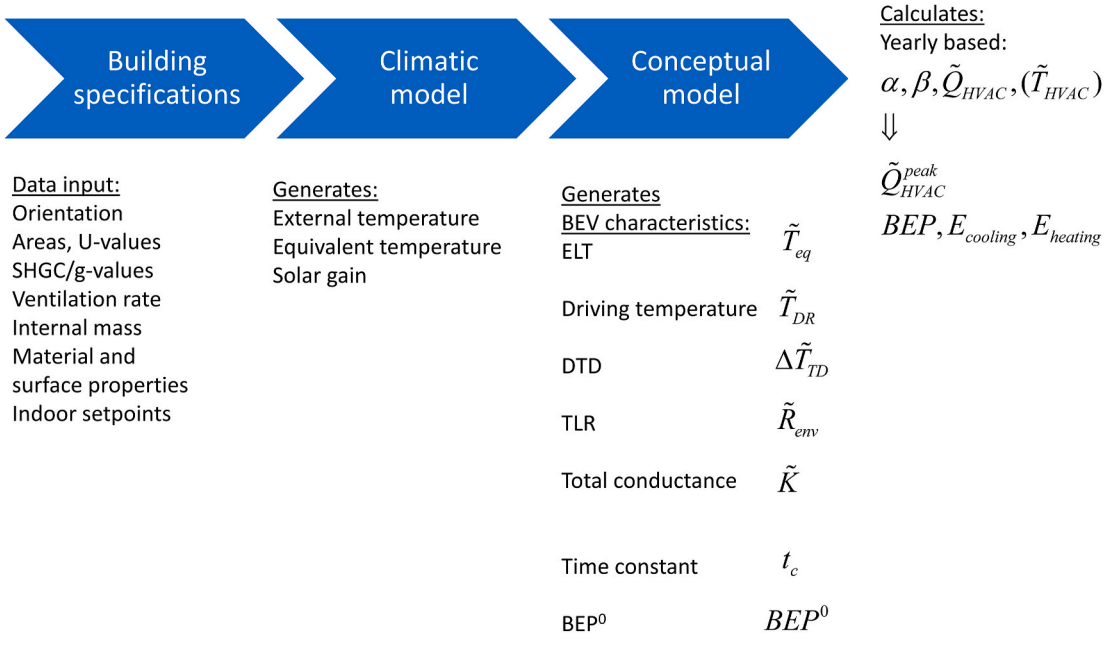

Fig. 22. Workflow sketch for using the Conceptual model.

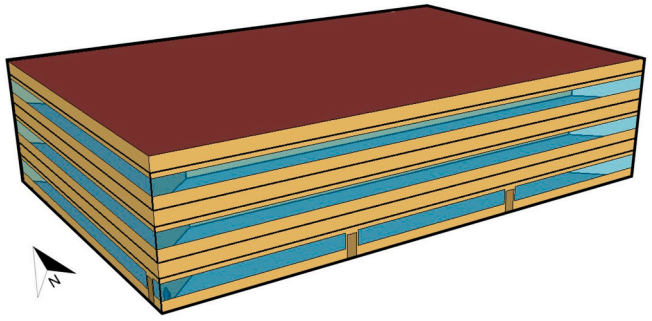

Fig. 23. DOE prototype medium office building [28].

$$BEP = \alpha \cdot BEP^0 = 0.5052 \cdot 101.7 = 51.4 \ \text{kWh/m}^2$$

$$BEP^C = \beta \cdot BEP = 0.1564 \cdot 51.4 = 8.0 \ \text{kWh/m}^2$$

The peak loads are 141 kW for heating and 83 kW for cooling.

This case generated a small increase, 2%, in the energy demand (0.8 kWh/m^2), while the cooling demand was reduced by 31%, (3.6 kWh/m^2).

6. Conclusions

A simplified model for the energy balance of a building, the Conceptual model, is developed, tested, and demonstrated. It is based on a network model and lumped analysis of the dynamic process. Solution techniques using stable explicit forward differences based on analytical solutions are derived.

Characteristic parameters for the buildings are introduced; Driving temperature (DT), Driving temperature difference, (DTD), External Load Temperature (ELT), Thermal Load Resistance (TLR). DT represents the overall exterior and interior climatic influences on the building in temperature degrees. Further, DTD is the annual average and absolute difference between the average indoor temperature and DT. ELT is a fictitious external temperature defined by the exterior surface temperature and air infiltration. Finally, TLR is an effective thermal resistance of the whole building envelope, including the effect of air infiltration.

The Building Envelope Performance, BEP^0-value (J/m^2[Btu/ft^2]) is introduced in this paper, representing the overall thermal performance of the building while the indoor temperature remains constant. BEP^0 is used together with *BEP*(overall thermal performance of the building envelope when the indoor temperature is allowed to float within given thermostat setpoint temperatures) to determine an energy demand factor, α. In addition, using *BEP*, the ratio of cooling over the overall heating and cooling demand, β, is introduced.

The conceptual model has been used for mapping DTD, α and β for two DOE prototype buildings; large hotel and medium office. The three parameters have been visualized on U.S. maps and for each building type, which allows to communicate the heating and cooling demand and their relation to building characteristics, in a concise way. According to these maps, DTD is the lowest in East-Southern areas of the U.S., as well as in West coast climates. α, which basically describes the potential of utilizing a building's thermal mass while allowing the indoor temperature to float, indicates that thermal mass have the largest impact on the overall energy demand in states like California, Florida, and Southern areas of Alabama and Georgia.

This paper also presents the correlation between thermal mass (through a time constant) and the thermostat setpoint deadband on the overall energy demand. According to the analysis, there is strong positive correlation between these two variables, and one could argue that there is a present "symbiosis" between the two. If one cease to exist, the positive impact on the overall energy demand halts.

Declaration of competing interest

The authors declare that they have no known competing financial interests or personal relationships that could have appeared to influence the work reported in this paper.

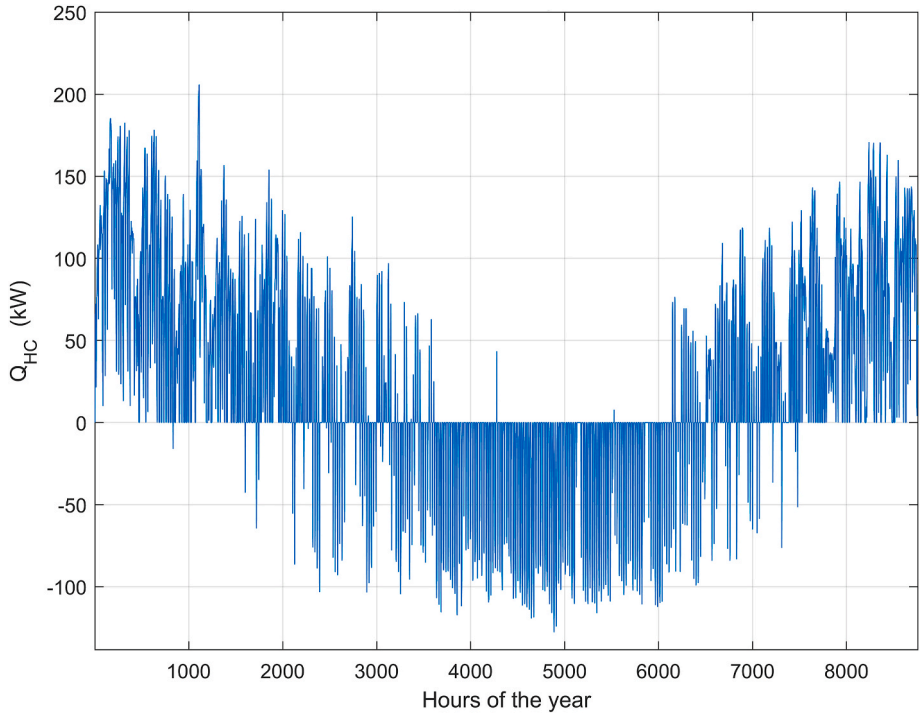

Fig. 24. Heating and cooling demand for a "Medium Office" building in Athens, Georgia during the course of a year.

Nomenclature (SI-units)

a	Thermal diffusivity (m^2/s)
A	Area (m^2)
BEP	Building envelope performance (J/m^2)
c	Heat capacity of building material (J/kg,K)
c_{pa}	Heat capacity of air at constant pressure (J/kg,K)
d	Thickness (m)
DTD	Driving temperature difference (˚C)
E	Energy demand (J or kWh)
ELT	External Load Temperature (˚C)
i,j	Index (−)
K	Conductance (W/K)
m	Mass (kg)
M	Interior thermal mass (kg)
Q	Heat flow (W)
R_a	Air infiltration rate (m^3/s)
$\tilde{R}_{env}$	Thermal load resistance, effective thermal resistance of the whole building envelope per unit area (m^2K/W)
t_c	Characteristic time constant for building (s)
t_p	Time period for periodic process (s)
t_{year}	Time span of one year (s)
T	Temperature (˚C)
TLR	Thermal Load Resistance (m^2K/W)
$\overline{T}_i$	Mid setpoint temperature (˚C)
U	U-value of envelope part (W/m^2K)

Greek symbols

α	Ratio between energy demand when thermal comfort interval is greater than zero and zero (−)
β	Ratio of cooling over the overall heating and cooling demand (−)
ΔT	Temperature deadband width/total span of thermal comfort interval (˚C)
ΔT_{in}	Fictitious increase in external temperature due to solar and internal gains (˚C)
ρ_a	Density of air (kg/m^3)

Subscript

A	Amplitude
DR	Driving (temperature)
e	Exterior

env	Envelope
eq	Equivalent
free	Free running temperature, i.e. without heating or cooling
i	Interior
gain	Gain due to internal sources of heat
HC	Heating or Cooling
p	Periodic process
sol	Solar related heat gains
t	Transmission
v	Ventilation by air infiltration
W	Window

Superscript

0	Base case
ˆ	Notation (tilde) for variable used for the Conceptual network model

Appendix A

A.1 Numerical accuracy – Internal step in heat gain.

In this subsection, the accuracy of the network reduction presented in Fig. 6 (right) is analyzed by comparing the resulting heat balance with the less accurate methods given in Fig. 4. Four building types are simulated to compare the result between the two methods. They all correspond to a floor unit in a multi-story building with the characteristics given in Table 6.

Table 6
Simuated building properties.

Floor Area	100 m^2	1076.39 ft^2
Wall Length	10 m	32.8 ft
Floor Plane Height	3 m	9.8 ft
Window-to-Wall Area	15%	15%
Window U-factor	1.5 W/m^2K	0.26 Btu/hr,ft^2,°F
Opaque Wall U-value	0.25 W/m^2K	–
Opaque Wall *R*-value	–	22.7 h,ft^2,°F/Btu
Wall Insulation – Density	70 kg/m^3	4.37 lb/ft^3
Wall Insulation – Thermal Conductivity	0.035 W/mK	0.02 Btu/hr,ft,°F
Wall Mass Thickness – Heavy (Concrete)	0.1 m	4 inches
Wall Mass Thickness – Light (Dry Wall)	0.026 m	1 inch
Floor Mass Volume – Heavy (Concrete)	10 m^3	353 ft^3
Floor Mass Volume – Light (Joist)	0.004/m^2	0.075/ft^2
Internal Mass from furniture (Wood)	1 m^3	35.3 ft^3
Exterior heat transfer surface coefficient	0.04 m^2K/W	0.007 Btu/hr,ft^2,°F
Interior heat transfer surface coefficient	0.13 m^2K/W	0.023 Btu/hr,ft^2,°F
Air Exchange Rate	0.5 h^{-1}	0.5 h^{-1}

Combinations of light and heavy buildings are considered, with respect to thermal mass of both walls and floor. All four buildings simulated are box-shaped. The exterior part of the wall consists of mineral wool and the inner wall layer consists of either concrete (heavy mass) or two layers of gypsum board (light mass). The effect of the timber frame is neglected. An adiabatic symmetry plane is assumed in the middle of the floors.

The core dynamics are covered by a step change in the heat released to the interior node.

The initial interior temperature and the external equivalent temperatures are zero. The released ΔQ_{HC}(and $\Delta \tilde{Q}_{HC}$) is chosen so that the final steady-state temperature becomes one.

$$\Delta Q_{HC} = \tilde{K} \cdot H(t) \tag{37}$$

Here, *H(t)* is the Heaviside unit step function.

The numerical analysis is done in MATLAB® using the ode45 solver for system of ordinary differential equations and using two methods.

- Comprehensive method (Fig. 4)
- Simplified/Conceptual method – Combined envelope and interior mass (Fig. 6, right)

The FDM scheme uses 30 computational cells for the wall, 20 in insulation and 10 in the inner layer of the concrete or gypsum. An additional computational cell represents the lump. The result from using the comprehensive method is given by black curves in Fig. 25 and Fig. 26. The problem with a number of thermal masses connected as in Fig. 4, is described in previous work [25]. Using the thermal coupling matrix and the corresponding eigenvalues, the maximum time scale, t_c, of the system can be found.

Here, $\tilde{K} = 104.58$ W/K [$\tilde{K} = 1.9$ Btu/hr,°F]. The result is presented as green curves in Figs. 25 and 26.

For the conceptual model, a part of the building envelope mass (gypsum or concrete) interior of the insulation is added to the interior mass, generating a time scale as:

$$T_i'(t) = 1 - e^{-t/t_c} \tag{38}$$

$$t_c = \frac{cM}{\tilde{K}} \tag{39}$$

$$cM = cM_0 + \rho c_{wall} A_{wall} d_{innerwall\ \ layer} \tag{40}$$

Here, $\tilde{K} = 104.58$ W/K [$\tilde{K} = 1.9$ Btu/hr,°F]. The result is presented as green curves in Figs. 25 and 26.

The result is shown as green curves in Figs. 25 and 26.

Table 7
Time scale for the four cases, defined by the FDM analysis (eigenvalues) and (2) (39).

Case	t_c(h) (eigenvalues)	t_c(h)
I - Light wall/Heavy floor	16.6	16.1
II - Heavy wall/Heavy floor	105.3	104.9
III - Light wall/Light floor	6.9	6.2
IV - Heavy wall/Light floor	59.1	55.2

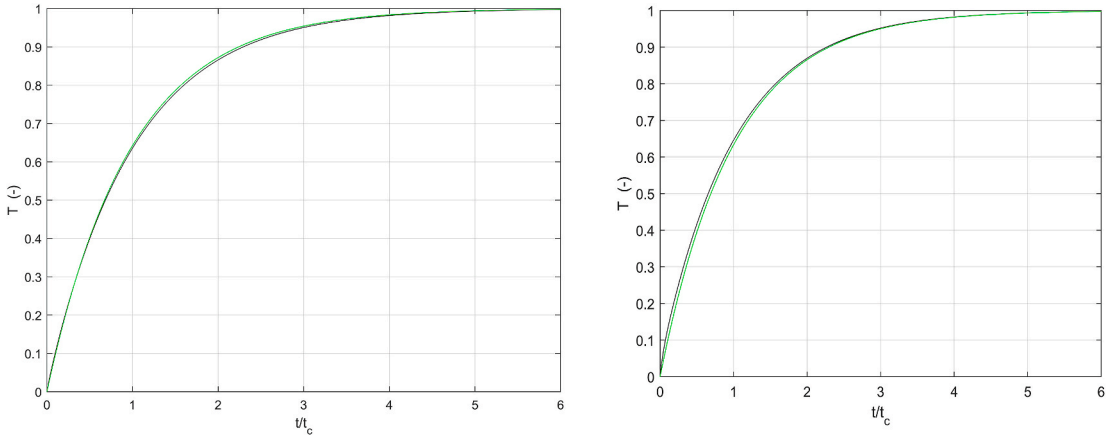

Fig. 25. Interior temperature response due to a step change in the interior heat source for Case I (left) and Case II (right).

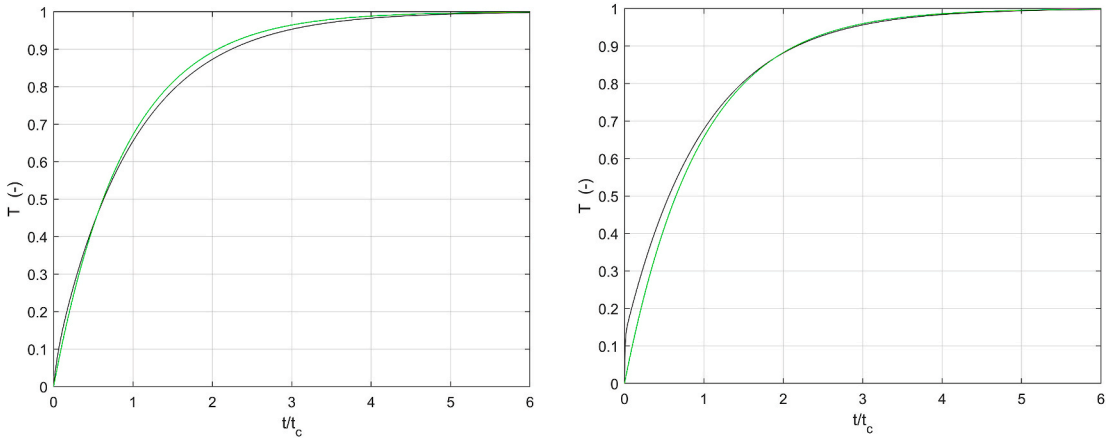

Fig. 26. Interior temperature response due to a step change in the interior heat source for Case III (left) and Case IV (right).

Case I corresponds to a light wall and heavy floor. The maximum absolute error is 0.0073 occurring at $t/t_c = 1.32$.

Case II, Fig. 25 (right), corresponds to heavy wall and heavy floor. The absolute error is 0.032 occurring at $t/t_c = 0.12$.

Case III corresponds to light wall and light floor. The absolute error is 0.0328 occurring at $t/t_c = 0.1$. The error becomes zero and change sign at $t/t_c = 0.553$ and reach a new local maximum of 0.0213 at $t/t_c = 1.5$.

Case IV corresponds to heavy wall and light floor. The maximum absolute error is 0.1171 at times close to zero, at $t/t_c = 0.5$ it reduces to 0.055, and at $t/t_c = 1$, the error is 0.021. Case IV gives the greatest error of all cases. In the FDM solution there is a fast response at small times. The effect, ΔQ_{HC}, that is applied from time zero to the interior thermal mass, gives a fast increase in temperature while the major part of the wall thermal mass increases much slower.

A.2 Step change in exterior temperature.

Using the conceptual model, step changes in the equivalent temperature govern the heat flow to and through the wall and roof to the interior without accounting for its thermal mass. The effect of this will be analyzed now in this subsection.

Solar and internal gain as well as heating and cooling is neglected here. The analysis is focused on the heat transfer through the opaque walls only.

FDM solutions are used for comparisons. The previously defined cases (I through IV) will be used. The driving temperature is normalized to unity and the time is scaled with t_c, in accordance with Eq. (43). The results for all four cases are presented in Fig. 27. Here, the most accurate results are given by the numerical model and presented in black. The results from the conceptual model are depicted in green.

The step change in driving temperature for the conceptual model (without solar gains) is:

$$\tilde{T}_{DR} = \tilde{T}_{eq} = \frac{K_{wall} \cdot H(t) + K_W \cdot 0 + K_v \cdot 0}{\tilde{K}} = \frac{K_{wall}}{\tilde{K}} H(t) \tag{41}$$

The step response solution, $T_{st}(t)$, for the interior temperature is given by:

$$\frac{T_{st}(t)}{\tilde{T}_{DR}} = \left(1 - e^{-t/t_c}\right) \cdot H(t) \tag{42}$$

$$t_c = \frac{cM}{\tilde{K}} \tag{43}$$

The largest error is obtained for case III with both a light mass wall and floor. The maximum absolute error in the normalized curve is then 0.2 at t/t_c, approximately equal to 0.4. For t/t_c less than 0.1 and greater than 1.44, the error is less than 0.10. There is a typical smaller delay between the two responses. The conceptual model does not account for any thermal mass of the wall in the calculation of the heat flow inwards. All mass has been moved into the lump, so the response is faster for the conceptual model, and consequently does not account for the delay caused by the wall heat capacity. Still, it will be correct in terms of transferred energy over longer times since the U-values are accounted for properly. The delay in the change of the interior temperature due to the wall response will be less pronounced for the whole-building response when also the heat transfer through windows, ventilation and solar gains are accounted for.

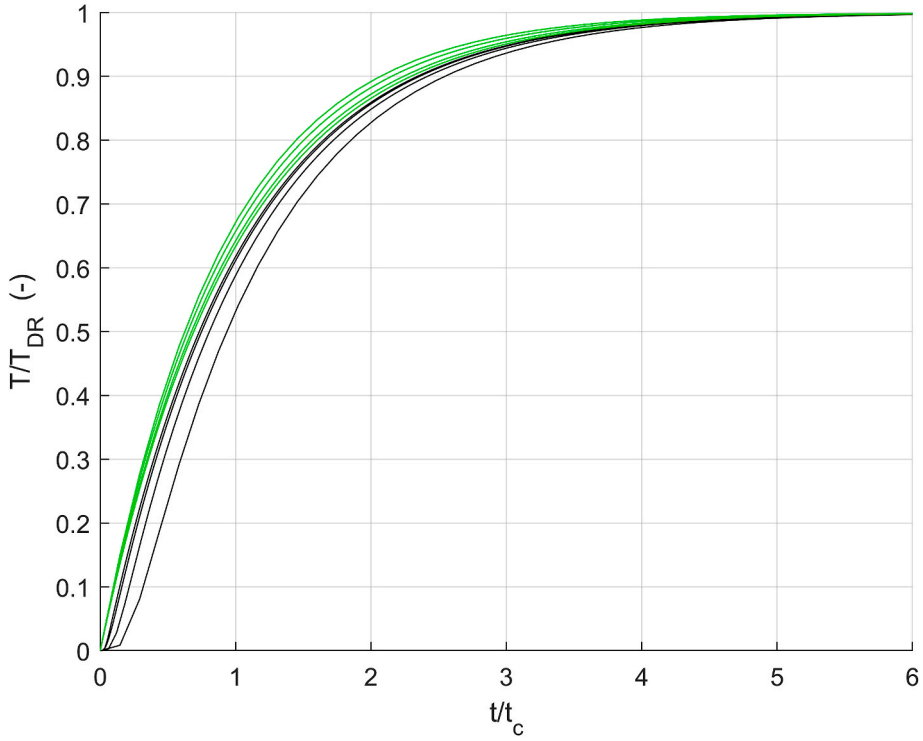

Fig. 27. The interior temperature response after a step change in the equivalent external temperature (outside the wall). Numerical results (black) and conceptual model approximation (green) for the four cases. (For interpretation of the references to colour in this figure legend, the reader is referred to the Web version of this article.)

A.3 Synthetic weather data year.

As an additional test for the conceptual model (compared to FDM), the four cases will be investigated for a synthetic weather case.

The exterior temperature and the heat gains are assumed varying as:

$$T_e = 10 + 10 \cdot \sin\left(2\pi t \,/\, t_{p,year}\right) + 5 \cdot \sin\left(2\pi t \,/\, t_{p,day}\right) \tag{44}$$

$$T_{eq} = 10 + 10 \cdot \sin\left(2\pi t \,/\, t_{p,year}\right) + 15 \cdot \sin\left(2\pi t \,/\, t_{p,day}\right) \tag{45}$$

$$Q_{sol} = 1000 \cdot \left(1 + \sin\left(2\pi t \,/\, t_{p,year}\right)\right)/2 + 4000 \cdot \left(1 + \sin\left(2\pi t \,/\, t_{p,day}\right)\right)/2 \tag{46}$$

The starting temperature is zero and the total conductance $\tilde{K} = 104.58$ W/K [$\tilde{K} = 1.9$ Btu/hr,°F].

The results are presented in Table 8 and Fig. 28 and Fig. 29.

Table 8
Error in the free running temperature for the conceptual model in comparison with the FDM results. The absolute mean difference is less than 0.02 °C and the greatest standard deviation is between 0.33 and 1.87 °C.

Case	Absolute mean difference (°C/°F)		Standard deviation (°C/°F)	
I (Light wall Heavy floor)	0.006	0.011	0.33	0.59
II (Heavy wall Heavy floor)	0.02	0.036	0.34	0.61
III (Light wall Light floor)	0.001	0.0018	0.83	1.5
IV (Heavy wall Light floor)	0.009	0.016	1.87	3.4

The main difference between the numerical model and the conceptual one is in the daily amplitude. For Case II, with the heavy wall, the conceptual model diurnal amplitude is 1.04 instead of 1.37, i.e. 24% smaller than from calculation using FDM. For Case IV, with the heavy wall, the conceptual model diurnal amplitude is 1.83 instead of 3.4, i.e. 44% smaller than FDM results. For case IV, the interior mass is dominated by the wall thermal mass.

For Case I and III, the conceptual model daily amplitude is only between 5 and 7% greater.

For the studied cases with a free running temperature, the interior temperature varies greatly between day and night. This means that the interior interaction with the thermal mass of wall and floor has a great impact on the indoor temperature amplitude. For case IV, the diurnal penetration depth is in the order of the wall thickness. The active mass, i.e. the part of the wall mass that is active in the load and unload of heat during cycling of temperatures is somewhat reduced. However, in climates with predominating heating or cooling, this will impact the results less. For this reason, the required energy for heating and cooling was also tested. The upper comfort interval is 24 °C and the lower one is 22 °C. Table 9 compares the calculated energy for cooling and heating between the FDM and conceptual models.

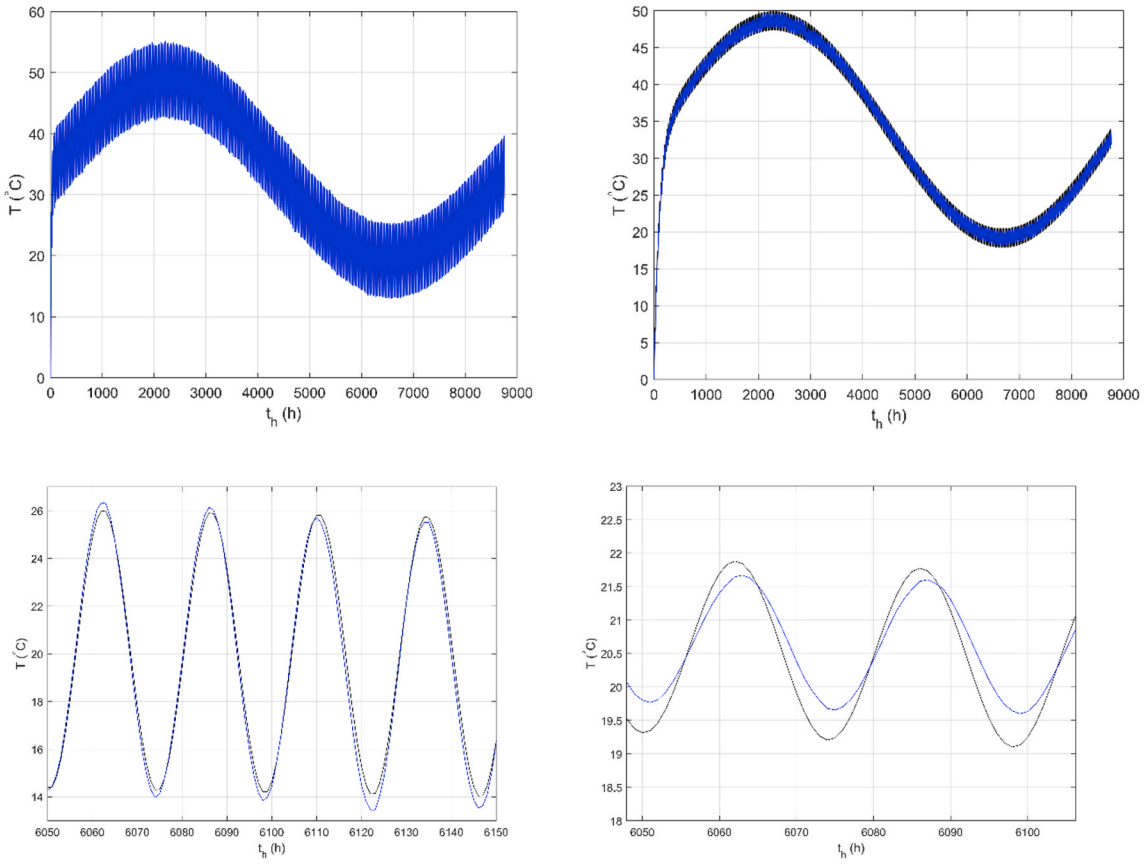

Fig. 28. Comparisons between numerical FDM model and the conceptual model during a year (above) and a few days (below) for Case I (left) and II (right).

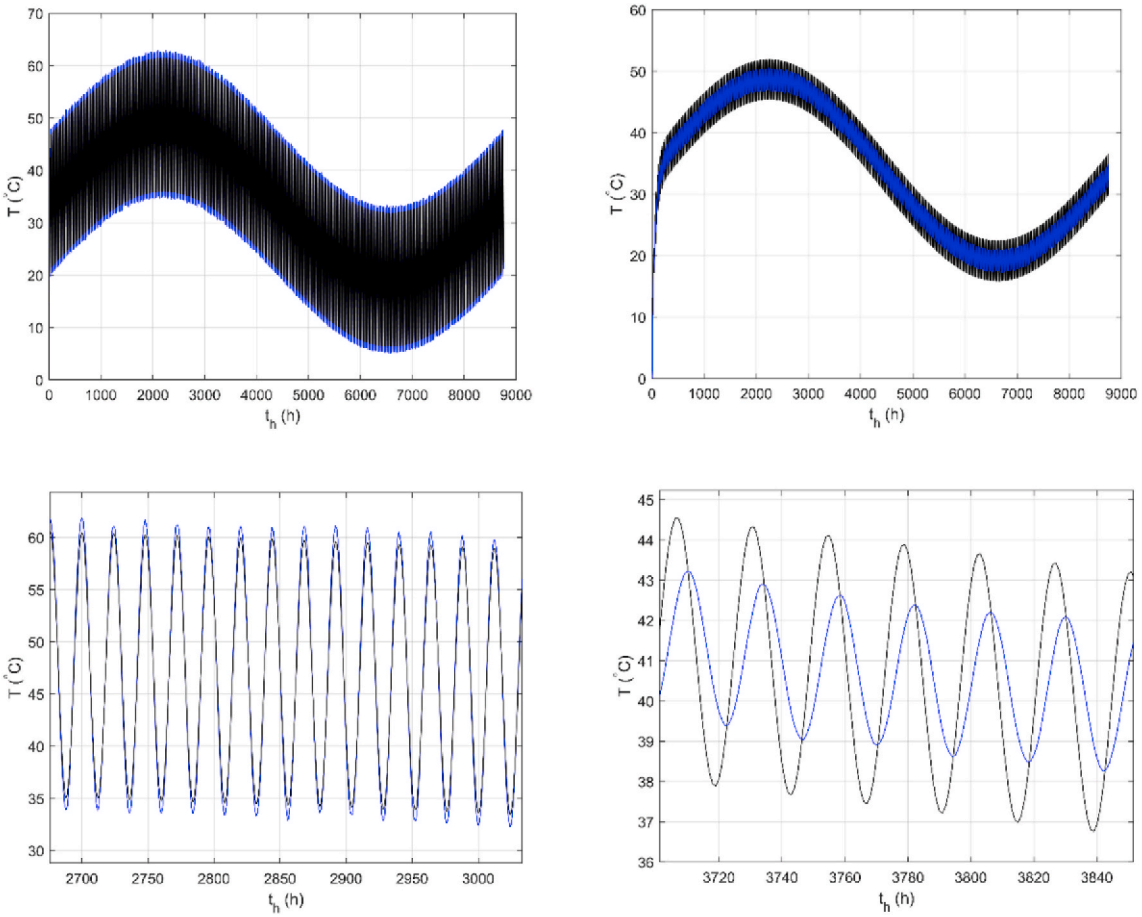

Fig. 29. Comparisons between numerical FDM model and the conceptual model during a year (above) and a few days (below) for Case III (left) and IV (right).

Table 9
Calculated energy for cooling and heating during a year using the FDM and the conceptual model.

Case	FDM (MWh/MBtu)				Conceptual model (MWh/MBtu)			
	Cooling		Heating		Cooling		Heating	
I (Light wall Heavy floor)	12.52	42.72	2.87	9.79	12.46	42.52	2.99	10.20
II (Heavy wall Heavy floor)	10.15	34.63	0.64	2.19	10.03	34.22	0.50	1.71
III (Light wall Light floor)	13.02	44.43	3.35	11.43	13.17	44.94	3.49	11.91
IV (Heavy wall Light floor)	11.32	38.63	1.75	5.97	11.02	37.60	1.49	5.08

The analyzed case is dominated by a cooling demand. The maximum error between the models in this case is less than 3%. For the heating demand, which is quite small compared with the cooling demand, the error is maximum 22% for Case II and for the other cases; 4 and 18% respectively. The absolute error is maximum $0.142 \cdot 10^3$ kWh for Case II and 0.12, 0.14 and $0.31 \cdot 10^3$ kWh for the other three cases.

References

[1] F.C. McQuiston, J.D. Parker, J.D. Spitler, Heating, Ventilating, and Air Conditioning: Analysis and Design, John Wiley & Sons, 2004.
[2] Arkar, C., & Perino, M. (2019). Dynamic Thermal Performance Metrics for Adaptive Building Constructions. Paper presented at the 16th IBPSA International Conference and Exhibition, Rome.
[3] P. Scott West, B. Beap, P. Bemp, Energy simulation aided design for buildings, ASHRAE J. 61 (12) (2019) 20–26.
[4] J. Spitler, F. McQuiston, K. Lindsey, CLTD/SCL/CLF Cooling Load Calculation Method, 1993. Paper presented at the the 1993 Winter Meeting of ASHRAE Transactions. Part 1, Chicago, IL, USA, 01/23-27/93.
[5] EnergyPlus, Engineering Reference - the Reference to EnergyPlus Calculations, 2019. Retrieved from, https://energyplus.net/sites/default/files/pdfs_v8.3.0/EngineeringReference.pdf.
[6] Building Envelope Campaign, Retrieved from, https://ec.ornl.gov/, 2020.
[7] K. Childs, Appraisal of the M factor and the role of building thermal mass in energy conservation, NASA STI/Recon Technical Report N, 1980, p. 80.
[8] T. Kalamees, IDA ICE: the simulation tool for making the whole building energy and HAM analysis, Annex 41 (2004) 12–14.
[9] K. Lengsfeld, A. Holm, Entwicklung und Validierung einer hygrothermischen Raumklima-Simulationssoftware WUFI®-Plus, Bauphysik 29 (3) (2007) 178–186.
[10] J.E. Christian, J. Kosny, Thermal performance and wall ratings, ASHRAE J. 38 (3) (1996).
[11] S. Ferrari, V. Zanotto, Approximating dynamic thermal behaviour of the building envelope, in: S. Ferrari, V. Zanotto (Eds.), Building Energy Performance Assessment in Southern Europe, Springer International Publishing, Cham, 2016, pp. 21–33.
[12] A. Reilly, O. Kinnane, The impact of thermal mass on building energy consumption, Appl. Energy 198 (2017) 108–121, https://doi.org/10.1016/j.apenergy.2017.04.024.
[13] D. Alterman, T. Moffiet, S. Hands, A. Page, C. Luo, B. Moghtaderi, A concept for a potential metric to characterise the dynamic thermal performance of walls, Energy Build. 54 (2012) 52–60.
[14] P.W. O'Callaghan, S.D. Probert, Sol-air temperature, Appl. Energy 3 (4) (1977) 307–311, https://doi.org/10.1016/0306-2619(77)90017-4.

[15] Masonry Industry Committee, The "m" Factor: the Use of Mass to Save Energy in Heating and Cooling of Buildings, Retrieved from Masonry Industry Committee, 1978.
[16] H.C. Yu, The M Factor: A New Concept in Heat Transfer Calculations, Consulting Engineer, 1978.
[17] S.S. Moody, D.J. Sailor, Development and application of a building energy performance metric for green roof systems, Energy Build. 60 (2013) 262–269.
[18] K. Childs, Appraisal of the M factor and the role of building thermal mass in energy conservation, NASA STI/Recon Technical Report N, 1980, p. 80.
[19] R.D. Godfrey, K.E. Wilkes, A.G. Lavine, A technical review of the M factor concept, ASHRAE J. 22 (3) (1980) 47–50.
[20] R.D. Godfrey, K.E. Wilkes, A.G. Lavine, A Technical Review of the, 2016. *M" Factor Concept.* Paper presented at the Buildings XIII Conference, Atlanta.
[21] ASHRAE, ASHRAE Handbook of Fundamentals - Chapter 18 - Nonresidential Cooling and Heating Load Calculations, American Society of Heating, Refrigerating and Air Conditioning Engineers, NY, 2017.
[22] ASHRAE, ASHRAE Standard 90 Project Committee - Energy Conservation in New Building Design, American Society of Heating, Refrigeration and Air Conditioning Engineers, Inc., Atlanta, GA, 1975. ASHRAE Standard: 90-1975.
[23] F.W.H. Yik, K.S.Y. Wan, An evaluation of the appropriateness of using overall thermal transfer value (OTTV) to regulate envelope energy performance of air-conditioned buildings, Energy 30 (2005) 41–71.
[24] Heating, A. S. o., Refrigerating, Engineers, A.-C., America, I. E. S. o. N., Energy Efficient Design of New Buildings except Low-Rise Residential Buildings, vol. 90, ASHRAE, 1989.
[25] C.-E. Hagentoft, S. Pallin, Thermal step response of N-layer composite walls—accurate approximative formulas, J. Heat Tran. 142 (3) (2020).
[26] S. Pallin, J. DeGraw, M. Bhandari, T. Pilet, Quantifying Thermal Performance of the Building Envelope - beyond Common Practice, 2020. Paper presented at the XV International Conference on Durability of Building Materials and Components - DBMC 2020, Barcelona.
[27] S. Pallin, C.-E. Hagentoft, A. Aldykiewicz, M. Bhandari, Development of a Simplified Methodology for Building Envelope Thermal Characterization, 2020. *Journal of Building Performance Simulation* , Submitted for review July 2020.
[28] EnergyCodes, Commercial Prototype Building Models, 2020. Retrieved from, https://www.energycodes.gov/development/commercial/prototype_models.
[29] R. Perez, P. Ineichen, R. Seals, J. Michalsky, R. Stewart, Modeling daylight availability and irradiance components from direct and global irradiance, Sol. Energy 44 (5) (1990) 271–289.
[30] ASHRAE, Fundamentals, Chapter 16 - Load and Energy Calculations - Ventilation and Infiltration, American Society of Heating, Refrigerating and Air-conditioning Engineers, Inc, Atlanta, GA, 2017.
[31] S. Medved, B. Černe, A simplified method for calculating heat losses to the ground according to the EN ISO 13370 standard, Energy Build. 34 (5) (2002) 523–528.
[32] F. Ståhl, *Influence of Thermal Mass on the Heating and Cooling Demands of a Building Unit*. Doctoral Thesis, Chalmers University of Technology, Sweden, 2009, ISBN 978-91-7385-350-7.
[33] IECC, International Energy Conservation Code - Residential Energy Efficiency, Internation Code Council, Inc, USA, 2012. Country Club Hills, IL.
[34] https://www.rehva.eu/fileadmin/REHVA_Journal/REHVA_Journal_2016/RJ_issue_3/p.18/18-22_RJ1603_WEB.pdf, May, 2016.